Spatiotemporal distribution and microbial assimilation of polyamines in a mesotrophic lake

Krempaska, Natalia ; Horňák, Karel ; Pernthaler, Jakob

Abstract: We examined seasonal and spatial variations of dissolved free polyamines (DFPA) in the large mesotrophic prealpine Lake Zurich (Switzerland). An ion-pairing liquid chromatography method with mass spectrometric detection was optimized for the quantification of DFPA without prior concentration or derivatization. Total DFPA concentrations varied between 0.4 nM and 11 nM in winter and spring of 2015, respectively. Polyamine concentrations were highest in the epilimnion during the phytoplankton growth phase, and reflected occurrence patterns of diatoms. Putrescine consistently dominated the DFPA pool throughout the season whereas norspermidine was detected only once in spring. Incubations with 13C-labeled putrescine revealed concentration-dependent uptake rates (3.2–5 nM h–1) and short turnover times (2.4–4.4 h). In contrast, incorporation rates into biomass measured with 14C-labeled putrescine were substantially lower (0.9 nM h–1), indicating that this compound was predominantly respired. Uptake kinetics moreover suggested that putrescine in situ uptake rates were limited by low ambient concentrations. Competition assays revealed that putrescine uptake could only be inhibited by excess concentrations of another polyamine (spermidine), but not by amino acids. Bacteria affiliated with Limnohabitans and the acI lineage of Actinobacteria were identified as the taxa with the highest fraction (25–32%) of putrescine-incorporating cells. This compound was also utilized by Alphaproteobacteria, Cyclobacteriaceae, diatoms, and cyanobacteria. Overall, our data point to fast turnover of putrescine by different microorganisms, implying the importance of this substrate as an attractive energy source.

DOI: https://doi.org/10.1002/lno.10672

Spatiotemporal distribution and microbial assimilation of polyamines in a mesotrophic lake

Natalia Krempaska, Karel Horňák*, Jakob Pernthaler

Limnological Station, Department of Plant and Microbial Biology, University of Zurich, Kilchberg, Switzerland

Correspondence: khornak@limnol.uzh.ch

Phone: +41 (0)44 634 92 12

Fax: +41 (0)44 634 92 25

Running head: Polyamine variability and bacterial assimilation

Key words: Polyamines, spatiotemporal variability, freshwater bacteria, HPLC-mass spectrometry, uptake, turnover, transporter kinetics, bacterial assimilation, MAR-FISH, Actinobacteria, *Limnohabitans*

Abstract

We examined seasonal and spatial variations of dissolved free polyamines (DFPA) in the large mesotrophic prealpine Lake Zurich (Switzerland). An ion-pairing liquid chromatography method with mass spectrometric detection was optimized for the quantification of DFPA without prior concentration or derivatization. Total DFPA concentrations varied between 0.4 and 11 nM in winter and spring of 2015, respectively. Polyamine concentrations were highest in the epilimnion during the phytoplankton growth phase, and reflected occurrence patterns of diatoms. Putrescine consistently dominated the DFPA pool throughout the season whereas norspermidine was detected only once in spring. Incubations with ^{13}C-labeled putrescine revealed concentration-dependent uptake rates (3.2 – 5 nM h^{-1}) and short turnover times (2.4 – 4.4 h). In contrast, incorporation rates into biomass measured with ^{14}C-labeled putrescine were substantially lower (0.9 nM h^{-1}), indicating that this compound was predominantly respired. Uptake kinetics moreover suggested that putrescine in situ uptake rates were limited by low ambient concentrations. Competition assays revealed that putrescine uptake could only be inhibited by excess concentrations of another polyamine (spermidine), but not by amino acids. Bacteria affiliated with *Limnohabitans* and the acI lineage of Actinobacteria were identified as the taxa with the highest fraction (25 – 32 %) of putrescine-incorporating cells. This compound was also utilized by Alphaproteobacteria, Cyclobacteriaceae, diatoms and cyanobacteria. Overall, our data point to fast turnover of putrescine by different microorganisms, implying the importance of this substrate as an attractive energy source.

Introduction

Polyamines occur in every living cell and play an important role in various cellular processes, such as the stabilization of nucleic acids, transcription, translation, cell growth and proliferation, or the functioning of ion channels (Kusano et al. 2008). They also contribute to membrane stability and are involved in cellular stress responses (Tabor and Tabor 1985; Igarashi and Kashiwagi 2000; Jantaro et al. 2003). In aquatic systems polyamines are found in both, algae and bacteria (Hamana and Matsuzaki 1982, 1992). Phytoplankton exudation, viral lysis or grazing are among the key processes responsible for the release of dissolved free polyamines (DFPA) into the free water zone. Another important source of DFPA is the degradation of proteins and amino acids (Höfle 1984; Lu et al. 2014).

Current knowledge about the distribution, uptake, and fate of polyamines in aquatic systems is scarce, because most analyses of labile nitrogen-bearing organic compounds have been limited to amino acids. Only a few studies have examined DFPA concentrations in marine samples documenting that putrescine and spermidine typically dominate the DFPA pool (Lee and Jørgensen 1995; Nishibori 2001; Lu et al. 2014). However, DFPA concentrations and composition may temporarily change during phytoplankton blooms of diverse taxa (e.g. *Chatonella* spp., *Gymnodinium* spp.), when also unusual polyamines like norspermidine or caldopentamine could be present. These polyamines are mainly involved in growth regulation which is a function common to all polyamines (Nishibori and Nishijima 2004; Nishibori et al. 2009). The intracellular polyamine concentrations are usually at μM levels (Hamana and Matsuzaki 1982; Tabor and Tabor 1985) which contrasts their low sub-nM to nM amounts in ambient waters, with marked temporal and depth variations (Lee and Jørgensen 1995; Nishibori et al. 2003; Lu et al. 2014). The low DFPA concentrations could be explained by their efficient uptake via specific transport systems (Tabor and Tabor 1966;

Igarashi and Kashiwagi 1999). Polyamine uptake rates are similar to those of amino acids, but the fraction of polyamine-derived C assimilated by bacteria and the contribution of polyamines to bacterial C and N demands is typically lower than for amino acids (Höfle 1984; Liu et al. 2015). Planktonic microorganisms capable of DFPA utilization are not well characterized. Recent evidence from metagenomic data suggested that a substantial fraction of marine bacterioplankton, including *Roseobacter*- and SAR11-affiliated bacteria, Alpha-, Beta-, and Gammaproteobacteria, Actinobacteria and Flavobacteria, harbors genes for transport and degradation of polyamines (Moran et al. 2007; Mou et al. 2011; Ghylin et al. 2014).

DFPA in seawater have been previously determined by liquid chromatography after a one- or a two-step fluorometric derivatization (Nishibori 2001; Lu et al. 2014). Other methods based on liquid chromatography coupled to mass spectrometry (LC-MS) for the detection of underivatized polyamines have been applied in clinical (Häkkinen et al. 2013; Gosetti et al. 2013) or in food quality control applications (Gosetti et al. 2007; Sirocchi et al. 2014). None of the previous detection methods has been applied to and validated for freshwater samples.

The goals of our study were to adapt a previously described technique employing ion-pairing chromatography with mass spectrometric detection (Häkkinen et al. 2007) for the direct quantification of DFPA in lake water and to apply the optimized LC-MS method to examine the seasonal and spatial changes in DFPA concentrations in the large mesotrophic prealpine Lake Zurich (Switzerland). We also determined the uptake, incorporation and uptake kinetics of putrescine in short-term incubations with isotope-labeled tracers to assess its dynamics and importance to microbial consumers. Another objective was to investigate inhibition of putrescine uptake by a competition experiment with amino acids and another

polyamine to reveal uptake preferences of heterotrophic consumers for putrescine. Finally, we aimed to identify planktonic microbes involved in putrescine utilization by microautoradiography and fluorescence in situ hybridization (MAR-FISH). Based on previous studies (Moran et al. 2007; Mou et al. 2011; Ghylin et al. 2014), we hypothesized that putrescine will be assimilated by a broad range of planktonic bacteria.

Materials and methods

Reagents

Standard compounds 1,3-diaminopropane dihydrochloride (Dap, >98%), 1,5-diaminopentane dihydrochloride (Cad, >98%), 1,7-diaminoheptane (Dah, internal standard, >98%) and Bis(3-aminopropyl) amine (Nsd, >98%), N-(3-aminopropyl)-1,4-butanediamine trihydrochloride (Spd, ≥99.5%) and N,N′-Bis(3-aminopropyl)-1,4-butanediamine tetrahydrochloride (Spm, ≥99.5%) were purchased from Sigma-Aldrich. 1,4-diaminobutane dihydrochloride (Put, ≥99.0%) was obtained from Fluka. Structures of polyamines used in this study are shown in Suppl. Table 1. 1,4-^{13}C butanediamine dihydrochloride (^{13}C-Put) was from American Radiolabeled Chemicals, Inc. Heptafluorobutyric acid (HFBA, 99.5%), propionic acid (PrA, 99.5%) and formic acid (98%) were from Sigma-Aldrich. LC-MS grade acetonitrile (ACN) was from J.T. Baker, Avantor. Water used for preparation of solvents and standard stock solutions was purified in a Milli-Q Direct 8 system (Millipore).

Sampling

Water samples were taken biweekly from 4 February to 21 October 2015 at the deepest point of Lake Zurich, a large mesotrophic prealpine lake (406 m above sea level, area 65.06 km^2, max. depth 136 m, mean depth 51.7 m, residence time 440 d, 47°17'N, 8°36'E,

Switzerland) (Bossard et al. 2001). The samples were collected with a Friedinger sampler at depths of 0, 5, 10, 20, 30, 40, 60, 80 and 100 m. Depths were selected according to an ongoing long-term sampling campaign performed in Lake Zurich. Subsamples were filled in sterile 50 mL plastic tubes and kept in a closed isolated box until further processing. Sampling took place approximately at 10 a.m. and subsamples of 1 mL were filtered roughly 1 h later employing syringe filters (IC Acrodisc filter, 0.2 μm Supor membrane, PALL Life Sciences) pre-washed with 1 mL of Milli-Q water. Samples were stored at - 24°C in 2 mL glass vials (Glastechnik Gräfenroda) until analysis. In parallel, subsamples of 1 mL for bacterial abundance were fixed with formalin (final concentration, 2%), stained with 4',6-diamidino-2-phenylindole (DAPI; final concentration, 1 μg mL^{-1}) and quantified by flow cytometry (inFlux V-GS, Becton Dickinson) as described previously (Salcher et al. 2011). Vertical profiles of chlorophyll *a* (Chl *a*) concentrations were measured with a TS-16-12 fluoroprobe (bbe Moldaemke, Kronshagen, Germany). This multiple wavelength probe can determine different phytoplankton groups such as diatoms, chlorophytes, cryptophytes and the cyanobacterium *Planktothrix rubescens* based on different fluorescence excitation spectra of the mentioned phototrophic organisms (Beutler et al. 2002). For incubations with stable isotope and radiolabeled putrescine, samples from Lake Zurich were collected with a Friedinger sampler at 5 m depth into 1 L glass bottles on 24 and 30 September 2015, 18 March 2016, 27 April 2016 and 6 July 2016 (incubations I – V). Additional samples from the depth of 120 m were collected on 27 April 2016. Samples were kept at in situ temperature in the dark until further processing.

Furthermore, surface samples from different other lakes were collected only once to verify the recovery and performance of the HPLC-MS method on environmental samples of different matrix composition. The following lakes were sampled: Hüttnersee (eutrophic, 658

m above sea level, area 0.165 km^2, max. depth 13.3 m, mean depth 6.3 m, residence time 120 d, 47°14' N, 8°38' E), Türlersee (mesotrophic, 643 m above sea level, area 0.497 km^2, max. depth 22 m, residence time 730 d, 47°16' N, 8°30' E) (information obtained from Office of waste, water, energy and air, Canton Zurich, http://www.awel.zh.ch/internet/baudirektion/awel/de/wasser/messdaten/see_qualitaet.html). Thalwiler Waldweiher (eutrophic, 47°28' N, 8°56' E) and Seleger Moor (dystrophic, 47°25' N, 8°51' E).

Ion-pairing liquid chromatography

Polyamines were analyzed with an HPLC system (1260 Infinity series, Agilent Technologies) provided with a degasser, binary pump, autosampler and column oven. Analytes were separated on a YMC-Triart C-18 column (150 x 3 mm, 3 μm particle size, YMC) at a flow rate of 500 μL min^{-1}. Solvent A (Milli-Q water) and solvent B (ACN) were amended with 0.1% HFBA and 2% PrA. Samples of 100 μL and internal standard (Dah, final concentration 100 nM) were injected. A gradient elution started from 5% B to 50% B from 0 to 6 min, then 50% B was kept for 4.5 min, then 50-70% B from 10.5 to 10.6 min and 70% B was maintained for 3.4 min. Afterwards the gradient was returned from 70% to 5% B and column was re-equilibrated from 14.1 to 25 min. Column was thermostated at 35°C and samples were kept at 4°C during analyses. Prior to each measurement, column was equilibrated for 5 min at 95% A until the pressure was stable. Up to four blanks were run using the gradient elution above. Samples were amended with HFBA (final concentration 0.1 %) prior to HPLC-MS analyses.

Mass spectrometry

160 DFPA detection was carried out on an API 5000 triple quadrupole mass spectrometer
161 (AB Sciex) equipped with an electrospray ionization source and a QJet ion guide component.
162 During the multiple reaction monitoring scan (MRM) mode, polyamines were detected in the
163 positive ion mode. Tandem mass spectrometry (MS/MS) analyses were performed to select
164 for pairs of precursor and product ions (transitions) specific for each polyamine. Two
165 transitions with the highest signal intensity were selected per each analyte (only one
166 transition was used for Dap and Dah). Declustering potential (DP), entrance potential (EP),
167 collision energy (CE) and cell exit potential (CXP) parameters were further optimized for
168 each transition (Suppl. Table 2). EP was set for all transitions to 10 V. The lower *m/z*
169 threshold for all scans was set to 25. To optimize the ion source parameters, 0.1% HFBA and
170 100% ACN were applied isocratically (50%:50%) at the flow rate of 500 μL min^{-1}. Ion-spray
171 voltage (IS), temperature (TEM), along with curtain (CUR), collision (CAD) and ion source
172 gas (GS1 and GS2) parameters were optimized for highest signal intensities of the selected
173 transitions using the MRM scan mode. The outcome of the ion source optimization gave the
174 following setting: IS = 1500 V, TEM = 700°C, CUR = 10, CAD = 10, GS1 = 50, GS2 = 60.
175 Nitrogen was applied as curtain, collision and ion source gas. The dwell time was set to 100
176 ms for all transitions. Data was acquired with the software Analyst (version 1.6.1, AB Sciex)
177 and quantified by the MultiQuant software (version 2.1, AB Sciex) using the corresponding
178 extracted ion chromatograms.
179
180 *Method precision, limits of detection and quantification*
181 A calibration curve was established for each polyamine transition using dilution series
182 of aqueous stock solutions from 0.2 nM to 100 nM concentrations prepared from one stock
183 solution and the corresponding response factors were calculated using Dah as internal

184 standard. Prior to injection, dilution series of polyamine standards as well as environmental
185 samples were spiked with internal standard to yield a final concentration of 10 nM. Thus, a
186 constant internal standard concentration was maintained in all samples measured in this
187 study. Limits of detection (LOD) and limits of quantification (LOQ) were determined from
188 the calibration curves of the corresponding polyamine-transitions. LOD was determined as
189 the lowest analyte concentration yielding the signal to noise ratio >2 after correction for
190 blank. LOQ was determined as the lowest polyamine concentration yielding a relative
191 standard deviation of <10% obtained from the triplicate measurements. Method recovery was
192 determined in duplicate samples from different lakes (Lake Zurich, Hüttnersee, Türlersee,
193 Thalwiler Waldweiher, Seleger Moor) amended with ^{13}C-labeled Put at a final concentration
194 of 1 nM and 10 nM (Suppl. Table 3).
195
196 *Putrescine uptake and kinetics*
197 Triplicate samples amended with ^{13}C-Put at a final concentration of 10 nM and
198 duplicated controls without labeled putrescine were incubated for 4 to 5 h in the dark at in
199 situ temperature. Subsamples of 1 mL for quantification of DFPA by HPLC-MS taken at 1 h
200 intervals were filtered into glass vials using IC Acrodisc filters (0.2 µm, Pall) and stored at -
201 24°C. This was repeated for each incubation experiment (I-V) (Table 1). In addition, a
202 sample filtered through 0.8 µm filter (Nuclepore, Sterico AG) was incubated in parallel on 6
203 July 2016 to determine a contribution of free-living bacteria to the total Put uptake. Put
204 turnover time was calculated as the quotient of the total dissolved Put concentration and the
205 uptake rate. Kinetics of Put uptake was investigated on 18 March 2016 in triplicates of 100
206 mL taken from the depth of 5 m that were spiked with ^{13}C-Put to obtain final concentrations
207 of 1, 2, 5, 10, 20, 50 and 100 nM. Uptake rate was derived from differences in Put

concentrations after 2 h of incubation. Influence of other compounds on Put uptake was studied in another experiment performed on 18 March 2016. Samples of 100 mL were spiked with ^{13}C-Put (final concentration 10 nM) or with a mixture of ^{13}C-Put (10 nM) and either arginine, ornithine, or spermidine (100 nM each) (Table 1). The incubation period was 4 h and Put concentrations were quantified in 1 h intervals by LC-MS method described above. All incubations were performed at in situ temperatures in the dark. Samples were stored immediately after filtration at - 24°C until further measured.

Putrescine incorporation

For bulk incorporation rates triplicate samples of 10 mL were collected into sterile tubes and amended with [1,4-^{14}C] putrescine (^{14}C-Put, specific activity 110 mCi mmol^{-1}, incubations I-II) and [2,3-^{3}H] putrescine (^{3}H-Put, specific activity 60 Ci mmol^{-1}, incubations III-IV) from American radiolabeled chemicals to a final concentration of 10 nM. Duplicated controls prefixed with paraformaldehyde (PFA, final concentration 2%) were run in parallel. We used Put labeled with two radioisotopes because (a) incorporation rates measured with ^{14}C-tracer can be directly compared with total uptake rates measured with ^{13}C-Put samples, and (b) ^{3}H-tracer was found to be advantageous for microautoradiography analyses. All samples were incubated for 2 h in darkness at in situ temperature and subsequently fixed with PFA. Then, subsamples of 5 mL were filtered on 0.2 μm nitrocellulose filters (GSWP, diameter, 25 mm, Millipore) and processed as described by Kirchman (2001). Briefly, filters were washed twice with 5% ice-cold trichloroacetic acid and with 80% ice-cold ethanol to extract protein from microbial cells retained on a filter. Air-dried filters were placed into scintillation vials and dissolved in ethyl acetate. Afterwards scintillation cocktail (Rotoszint eco plus, LSC-Universalcocktail, Roth) was added and samples were analyzed with a

scintillation counter (Liquid Scintillation Analyzer, Tri-Carb 3170TR/SL, Perkin Elmer). Radioactivity (as disintegrations per minute) measured in samples corresponded to the amount of Put incorporated into microbial biomass over time. Differences between Put uptake rate (measured with ^{13}C-Put) and the corresponding incorporation rate (measured with ^{14}C-Put and ^{3}H-Put) were assumed to equal respiration (note that respiration was not directly measured). Put turnover time was calculated by dividing ^{13}C-Put concentration corrected for a natural Put pool by the corresponding uptake rate.

MAR-FISH

Samples of 10 mL were incubated with ^{14}C-Put (10 nM) or ^{3}H-Put (10 and 100 nM) for 2 h in the dark at in situ temperature and fixed as described for the bulk incorporation experiment. Then, the samples were filtered on 0.2 μm polycarbonate filters (GTTP, 25 mm diameter, Millipore) and washed twice with 1 mL of sterile pre-filtered deionized Milli-Q water (0.2 μm polycarbonate syringe filter, Whatman). CARD-FISH was performed according to Sekar et al. (2003) with the modifications of Neuenschwander et al. (2015). The following oligonucleotide probes were used: EUB338 I-III for most Bacteria (Daims et al. 1999), ALF968 for most Alphaproteobacteria (ALF) (Amann et al. 1997) and BET42a for most Betaproteobacteria (BET) (Manz et al. 1992), acI-853 for the acI lineage of Actinobacteria (acI) (Warnecke et al. 2005), LD12-115 for freshwater SAR11 (LD12) (Neuenschwander et al. 2015), R-BT065 for members of the genus *Limnohabitans* (RBT) (Šimek et al. 2001), PnecC-445 for *Polynucleobacter asymbioticus, P. duraque, P. yangtzensis, P. sinensis* (Hahn et al. 2009, 2016), LimA-23S-1435 for the LimA cluster of *Limnohabitans* (LimA) (Shabarova et al. 2017), LD2_739 for Saprospiraceae (LD2) (Pernthaler et al. 2004) and Cyc715 for Cyclobacteriaceae (Cyc) (Eckert et al. 2012).

Afterwards microautoradiography (MAR) was performed according to Alonso and Pernthaler (2005) with modifications described by Salcher et. al. (2008). Slides with hybridized bacterial cells were coated with a NTB emulsion (Carestream) and exposed for 1.5 to 2.5 d in the dark (Table 1). Emulsion was developed and fixed following manufacturer`s recommendations. MAR was performed in incubations I and II, whereas MAR coupled with CARD-FISH was conducted in incubations III and IV (Table 1). MAR-FISH preparations were evaluated with an epifluorescence microscope (Zeiss Axio Imager.M1) equipped with an automated microscopic platform. The option with multisport autofocus was chosen to provide a better focus of the cell layer on the agarose surface. Image quality control was applied to sort out low-quality images (Zeder et al. 2010). Between 500 and 2000 DAPI-stained cells captured from 8-10 images were analyzed per sample.

Results

Optimization of chromatographic conditions

HFBA as well as other volatile perfluorinated organic acids are readily used as ion-pairing reagents in reversed-phase chromatography to allow retention of polar analytes and to improve overall chromatographic performance (Kuhlmann et al. 1995; Gao et al. 2006; Häkkinen et al. 2007). In agreement with a previous study (Häkkinen et al. 2007) we found that HFBA enabled better separation and retention of polyamines than other tested ion-pairing agents (pentafluoropropionic and tridecafluoroheptanoic acid). Gradient elutions with different HFBA concentrations (0.025, 0.05, 0.1, and 0.5 %) were performed and analyzed. The length and mode of the gradient elution was further optimized by investigating different re-equilibration times and concentrations of ACN. We found that a linear ACN gradient with 0.1% HFBA was optimal for polyamine detection (Suppl. Fig. 1a).

Unfortunately the addition of perfluorinated acids often induces signal suppression of analytes during MS detection (Kuhlmann et al. 1995), as also observed in our method. This was substantially ameliorated by also adding propionic acid to both solvents according to previous reports (Kuhlmann et al. 1995; Häkkinen et al. 2007). The tested column showed markedly better separation performance if the elution started with 5% ACN, which was essential for obtaining symmetrical peak shapes and for reducing peak tailing or splitting. To ensure the stable chromatographic conditions and reproducible retention times between individual injections, the column was flushed with 70% ACN after the elution of polyamines to remove contaminants followed by a re-equilibration time of 10.9 min. Another key factor for improving the sensitivity of the method was the addition of HFBA (final concentration 0.1%) to samples prior to the analysis. The signal intensities of the analytes further increased, thus making the detection of sub-nM concentrations possible (Suppl. Table 2). Using the optimized LC-MS method, all 7 tested polyamines could be detected within 8 min (Suppl. Fig. 1a). Moreover, the co-eluting compounds Spd/Nsd and ^{12}C-Put/^{13}C-Put could be unambiguously quantified by their specific pairs of precursor and product ions (transitions).

Detection limits, recovery and signal interferences

Limits of detection (LOD) ranged between 0.2 - 0.5 nM and limits of quantification (LOQ) were between 0.5 - 5 nM (Suppl. Table 2). The detector response was linear at the lower range of concentrations (0.2 - 20 nM) for all tested polyamines, whereas a non-linear response was observed for Spd and Nsd at higher concentrations (50 - 100 nM), which was due to detector saturation (Suppl. Fig. 2). Recovery was determined as relative differences in the concentration of ^{13}C-labeled putrescine spiked into samples from freshwater habitats of different trophy and matrix complexity (Lake Zurich, Hüttnersee, Türlersee, Thalwiler

Waldweiher and Seleger Moor) compared to signals obtained in Milli-Q water. Recovery varied between 90 – 124 and 97 – 123 % at 1 and 10 nM levels, respectively (Suppl. Table 3). Tested polyamines revealed no major differences in signal intensities and background noise between the environmental samples, implying comparatively low detection limits. There were no remarkable interferences between the individual transitions monitored simultaneously. However, due to the applied mode of separation, i.e. no direct interaction between the column matrix and polyamines, there were signal interferences (likely HFBA adducts) detected for Nsd, Spd and Spm in blank samples (Milli-Q water). Nevertheless, these interferences could be substantially reduced after the optimization of the gradient including the column flushing step after the elution was accomplished. Other polyamines Dap, Put, ^{13}C-Put and Cad expressed low and stable background signal intensities in blanks.

Concentrations of individual polyamines and their spatiotemporal distribution

Total DFPA concentrations in Lake Zurich varied greatly between different periods of the season (Fig. 1a). DFPA concentrations were <2 nM in winter. The pool was dominated by Put, which was uniformly distributed throughout the water column with concentrations from <0.5 to 1.5 nM (Fig. 1a). DFPA concentrations markedly increased in spring with the absolute maximum (11 nM) detected in April. Put and Nsd quantitatively dominated the DFPA pool. DFPA concentrations gradually decreased with depth, but there were still approximately 2 nM detected in the depth of 100 m (Fig. 1b). In early summer the concentration pattern of the vertical profile was similar to that in spring, but Nsd was no longer detected in high quantities. Total DFPA concentrations increased to 6 nM (Fig. 1b). In late summer, vertical variations in DFPA concentrations resembled those in winter with total concentrations <2 nM (Fig. 1b). In autumn, there was an increase in DFPA concentrations

(up to 6 nM) and Put was the dominant component of the polyamine pool. However, the decrease in DFPA concentrations with depth was less pronounced than in summer since there were approximately 3 nM between 30 to 100 m (Fig. 1b). Overall, the spatio-temporal variations of Put concentrations tightly coincided with the total DFPA concentrations during the whole study period indicating that Put was the key polyamine in Lake Zurich.

Virtually the whole Chl *a* pool during this sampling campaign was constituted by the filamentous cyanobacterium *Planktothrix rubescens* with the maximum concentration of 30.3 μg Chl *a* L^{-1} by the end of August (Fig. 2a). *P. rubescens* was stratified in the metalimnion (approximately at 15 m) between May and October (Fig. 2a) which was below the depth of maximal DFPA concentrations (Fig. 1). The spatiotemporal distribution of *P. rubescens* tightly coincided with the period of a stable thermal stratification. Concentrations of diatoms were generally low with the maximum of 5.2 μg Chl *a* L^{-1} in the epilimnion recorded in June (early-summer). Diatoms were also detected between April and mid-May (spring) and from July to mid-August (late-summer) at concentrations of 3.4 and 2.9 μg Chl *a* L^{-1}, respectively (Fig. 2b). Total bacterial abundances ranged from 0.5 to 4.5 10^6 cell mL^{-1} with a maximum detected between mid-May and mid-June (Fig. 2c), which occurred just after periods of elevated DFPA concentrations (Fig. 1a). Bacterial abundances were substantially higher in the upper 20 m of the water column during stratification (mid-April to October).

Incubation experiments with labeled putrescine

Concentrations of labeled Put (^{13}C-Put) non-linearly decreased in all short-term incubation experiments (I-V, Table 1), implying that the tracer was actively utilized by microbes (Fig. 3). Uptake rates varied between 3.2 and 5 nM h^{-1} within the initial incubation period (0-2 h) (Fig. 3a, 3b), while those at the end of the incubation (2-5 h) ranged from 0.3

352 to 1 nM h^{-1}. The maximum Put uptake rate of 5 nM h^{-1} was detected on 6 July 2016
353 (incubation V) (Fig. 3c). Concentrations of non-labeled (natural) Put were mostly around 2
354 nM (incubation I-IV), while substantially elevated Put concentrations (12 nM) were found on
355 6 July 2016 (incubation V). Natural Put concentrations remained virtually constant with only
356 minor changes (0.4 – 1.5 nM) throughout the incubation periods (Fig. 3). Concentrations of
357 natural Put in treatments amended with labeled Put were indistinguishable from those in
358 controls without tracer additions and this was recorded in all incubations (Fig. 3). Total Put
359 incorporation rates, determined in parallel with the radiolabeled tracers, varied between 4 –
360 37 pM h^{-1} (^{3}H-Put) and 0.8 – 0.9 nM h^{-1} (^{14}C-Put) at the initial (0-2 h) incubation period.
361 Such a large discrepancy and the negligible ^{3}H-Put incorporation rates (<0.01 % of the Put
362 uptake rates measured with ^{13}C-Put) imply that ^{3}H-Put incorporation rates were apparently
363 underestimated. This could be potentially explained by a different fate or loss of the ^{3}H-label
364 during incubations. In comparison, ^{14}C-Put incorporation rates were 18 – 19 % of the
365 corresponding uptake rates suggesting that Put was mostly respired (Table 2), which is in the
366 range of previously published values (Liu et al. 2015). Put turnover times varied between 2.4
367 – 4.4 h.

368 Uptake kinetics of putrescine were examined in another incubation experiment (18
369 March 2016) using ^{13}C-Put. The ^{13}C-Put uptake rate changed with Put concentration (1 – 50
370 nM) according to a hyperbolic curve following the Michaelis-Menten kinetics (Johnson and
371 Goody 2011). Interestingly, the measured uptake rate at 100 nM concentration was markedly
372 higher and it could not be fitted by the hyperbolic curve (Fig. 4a). The maximal uptake rate
373 (V_{max}) and the half saturation constant (K_m) were 6.1 nM h^{-1} and 10.9 nM (Fig. 4b),
374 respectively. The effects of amino acids (Arg, Orn) and other polyamines (Spd) on the uptake
375 of Put were investigated in an experiment with epilimnetic water from Lake Zurich on 18

March 2016. Put concentrations decreased equally rapidly in treatments amended only with Put or with a mixture of Put and either Arg or Orn (Fig. 5). In contrast, the uptake of Put was inhibited by the excess amount of Spd (Fig. 5).

Identification of putrescine-incorporating cells

Despite measurable incorporation rates obtained with ^{14}C-Put in September 2015 (incubation I and II, Table 2), no cells with visible putrescine incorporation could be identified by MAR (data not shown). Therefore, ^{3}H-Put was used in incubations III and IV where on average 11.3 % of total DAPI-stained cells showed active Put incorporation (Fig. 6). The fraction of Put-incorporating cells was further identified by combining MAR with CARD-FISH (MAR-FISH, Figs. 6, 7). Both the acI lineage of *Actinobacteria* (acI) and the R-BT lineage of the genus *Limnohabitans* (R-BT) revealed the highest percentage (25 – 32 %) of Put-incorporating cells (Fig. 6). Betaproteobacteria (BET) and the acI lineage of Actinobacteria (acI) were the most abundant bacterioplankton components except for the deep water sample (120 m) from 27 April 2016 which was entirely dominated by BET. R-BT formed a large fraction of BET at the surface samples (5 m) and it showed a higher percentage of Put-active cells than BET. In contrast, the LimA lineage of the genus *Limnohabitans* (LimA) with relative abundances of 3 % revealed only a low fraction of Put-incorporating cells (4-8 %). Alphaproteobacteria (ALF) was the minor component of the community (3-4 %) but approximately 15 % of ALF incorporated Put at the surface, which was higher than the community average (Fig. 6). On the other hand, nearly no ALF incorporated Put in the sample from 120 m. Cyclobacteriaceae (Cyc) accounted for 4 – 8 % of the assemblage and their proportions of Put-active cells varied between 6 – 13 % (Fig. 6). Bacteria from other tested lineages such as the PnecC, LD12 and LD2 were found in very

low proportions (<2 %) and showed no visible Put incorporation (data not shown). In addition, *Asterionella sp*. (diatom) and *P. rubescens* (cyanobacterium) were also found to incorporate Put (Fig. 7e, h).

Discussion

Detection of DFPA in freshwaters

Our HPLC-MS method allowed direct detection of sub-nM concentrations of underivatized DFPA in diverse freshwater habitats at threshold concentrations that were comparable to or lower than previously reported ones (Nishibori 2001, 2003; Lu et al. 2014; Liu et al. 2015; Lu et al. 2015). The limits of detection of our method ranged between 0.05 - 0.5 nM (Suppl. Table 2), which is sufficiently sensitive for the accurate quantification of compounds at low to sub-nM levels in freshwater samples (Horňák and Pernthaler 2014; Horňák et al. 2016). Although Nsd and Spd could not be separated chromatographically, their unambiguous quantification was possible by mass spectrometry (MS) using the compound-specific pairs of precursor and product ions (transitions, Suppl. Table. 2). MS detection could, moreover, distinguish between natural Put and its isotope-labeled analog thereby providing a significant advantage over conventional fluorescence or pulse-amperometric detectors. The method also allows for a higher throughput (of 3 samples per hour) than reported previously (Nishibori 2001; 2003; Lu et al. 2014) and only requires addition of the ion-pairing reagent to samples prior to analysis. Despite the latter, the tested column maintained very stable and reproducible chromatographic conditions with low levels of background signal, allowing for the processing of large quantities of environmental samples without deterioration of detection quality.

424 *Spatiotemporal variations of DFPA in Lake Zurich*

425 This study provides a first spatiotemporal characterization of DFPA concentrations in
426 a natural freshwater system. The total DFPA concentrations in Lake Zurich are comparable
427 with those in seawater (Nishibori 2001; Nishibori et al. 2003; Lu et al. 2014; Liu et al. 2015)
428 and are substantially lower than in a eutrophic coastal salt pond (Lee and Jørgensen 1995).
429 Put and Spd usually dominate in coastal seawater (Badini et al. 1994; Nishibori 2001), while
430 other DFPA such as Nsd, Cad are reported only sporadically. This is in agreement with our
431 data (Fig. 1b): Put represented the quantitatively most important DFPA in all depths of Lake
432 Zurich throughout the study period, whereas Spm and Dap were consistently low (Fig. 1b).
433 Elevated concentrations of Nsd were only observed during spring (Fig. 1b, 15 April). Similar
434 to other polyamines, Nsd plays an improtant role in cell growth and development (Kusano et
435 al. 2008). Nsd was previously detected in seawater during a bloom of the dinoflagellate
436 *Gymnodinium* spp. (Nishibori et al. 2003). Members of this genus are also common in Lake
437 Zurich (Posch et al. 2015). Nevertheless, since no systematic analyses of the exudates of
438 different phytoplankton taxa were performed we can only speculate about the potential
439 source of Nsd in our samples.

440 Put concentrations in a coastal salt pond followed the pattern of primary production
441 (Lee and Jørgensen 1995), suggesting that actively photosynthesizing algae were the major
442 source of DFPA. In our study, the concentrations of total DFPA increased markedly in spring
443 (Fig. 1a), which coincided with increased diatom chl *a* concentrations (Fig. 2a). Higher
444 amounts of exudates are released during the spring phytoplankton bloom and these exudates
445 are a known source of polyamines (Höfle 1984; Lu et al. 2014). In addition, HPLC-MS
446 analyses confirmed the presence of large quantities of intracellular polyamines in cultures of
447 planktonic diatoms (genera *Gomphonema* and *Aulacoseira*), including isolates from Lake

448 Zurich (*Fragilaria sp.*) (Suppl. Fig. 1b). Thus, it is likely that DFPA in our study system were
449 at least partly derived from diatoms during spring.
450 However, the overall relationship between chl *a* (and, in turn, primary production) and
451 DFPA concentrations in Lake Zurich appears to be more complex (Figs. 1, 2). The
452 filamentous cyanobacterium *Planktothrix rubescens* is the dominant primary producer in
453 Lake Zurich (Bossard et al. 2001; Garneau et al. 2015). It stratifies in the metalimnion (at
454 approximately 12-15 m depth) from May to October (Fig. 2a) (Yankova et al. 2016) which is
455 below the depth of maximal DFPA concentrations. This species releases only negligible
456 amounts of extracellular products (Feuillade et al. 1990). It is, therefore, unlikely that DFPA
457 originated from *P. rubescens*. However, the presence of diatoms cannot account for the
458 increase in DFPA concentrations at the end of September (Figs. 1a, 2b), which might be
459 related to heterotrophic processes such as protein degradation (Höfle 1984), grazing or cell
460 lysis (e.g. Nagata 2000). On 9 April 2015 elevated DFPA concentrations of ~2 nM were
461 found in the hypolimnion (Fig. 1a), contrasting with the low concentrations of ~0.5 nM in the
462 remaining limnological year. This might be interpreted in the context of sedimentation of
463 senescent phytoplankton cells from the epilimnion and their subsequent decomposition in
464 deeper water layers (Grossart and Simon 1998).
465
466 *Uptake of labeled putrescine*
467 The concentration of ^{13}C- Put decreased non-linearly in all dark incubations (I-III and
468 V) (Fig. 3), implying that the Put uptake rate decreased proportionally to the concentration of
469 the tracer. These time-course changes in the uptake rate could be due to the upregulation of
470 membrane transporters, but might also result from differences between microbial populations
471 in the number of transporters and their respective saturation. Put uptake rates varied between

472 4.4 - 5 nM h^{-1} (incubations I, II, and V, Fig. 3) which is comparable to those in coastal
473 seawater, and higher than in open ocean waters (Liu et al. 2015). Concentrations of the tracer
474 substantially exceeded those of the natural Put in September 2015 (incubations I and II, Fig.
475 3a, b). Thus, our measurements reflected the potential (maximal) rather than the realized
476 uptake rates at that time point. By contrast, the concentrations of the labeled (tracer) and
477 natural Put were roughly equal in July 2016 (incubation V, Fig. 3c), suggesting that the
478 estimated Put uptake rate was likely close to the in situ one. Moreover, the concentration of
479 the natural Put pool remained stable over the course of the latter incubation, implying rapid
480 recycling (i.e., production) of this compound. Assuming that the natural and isotopically
481 labeled forms are consumed equally, the pool of dissolved Put at that time point was refilled
482 at a rate that was comparable to its uptake. Our detection method only targets dissolved free
483 polyamines (monomers) readily available to consumers. Therefore, despite stable
484 concentrations of ambient Put, it is unlikely that this Put pool was adsorbed to particles or
485 combined with other compounds which would preclude its consumption.
486 In September 2015 (incubations I and II, Table 2), approximately 20 % of the Put-
487 derived C taken up by organisms (measured by the ^{13}C-labeled tracer) was incorporated into
488 biomass (measured by the ^{14}C-labeled tracer), which is lower than in coastal seawater (Liu et
489 al. 2015), and than the fraction of C that is typically assimilated from amino acids (Crawford
490 et al. 1974, Jørgensen et al. 1983, Simon and Tilzer 1987). In July 2016 (incubation V, Suppl.
491 Fig. 3), the Put uptake rate in the size fraction <0.8 μm was 66% of the total rate in unfiltered
492 lake water, indicating that a major proportion of Put was taken up by free-living bacteria.
493 This agrees with observations of the consumption of dissolved carbohydrates and amino
494 acids (Weiss and Simon 1999). Nevertheless, the different uptake rates in the filtered and raw
495 lake water indicate that also larger microorganisms or bacteria attached to particles

contributed to Put uptake. However, we caution that the filtration through a polycarbonate membrane resulted in a substantial loss in the concentration of natural Put, which might have caused a bias in our rate measurements (Suppl. Fig. 3). Despite this potential artifact our results nevertheless indicate that the planktonic microbes in Lake Zurich readily consumed Put, as has been reported for marine bacteria (Höfle 1984; Liu et al. 2015). This was, moreover, confirmed by direct microscopic observation (Figs. 6, 7a-d).

Kinetics and inhibition of putrescine uptake

To avoid a non-linear decrease in Put uptake velocity potentially caused by experimental bias (i.e., compositional changes of the microbial assemblage due to prolonged incubation time, arbitrary concentration of the tracer, or down-regulation of membrane transporters) we performed a short-term (2 h) experiment in March 2016 (incubation III, Fig. 4) with different Put concentrations (1 – 100 nM). The relationship between Put concentrations up to 50 nM and uptake rate closely followed Michaelis-Menten kinetics (Johnson and Goody 2011) (Fig 4a). Therefore, Put uptake kinetics were similar to those of leucine and valine (Jørgensen 1992). By contrast, glucose consumption rates in Lake Zurich were constant at 10-30 nM concentrations (Horňák and Pernthaler 2014). In view of Put in situ concentrations (<2 nM), the estimated maximum Put uptake rate (V_{max}) of 6.1 nM h^{-1} and the corresponding half-saturation constant (K_m) of 10.9 nM indicate that uptake rates in Lake Zurich were strongly limited by Put availability (Figs. 1, 4a). This corroborates previous reports on the kinetic parameters of amino acid uptake (Burnison and Morita 1974; Bertilsson et al. 2007). Put uptake rate furthermore increased linearly between 1 - 10 nM, demonstrating that bacteria rapidly responded to the realized concentration maxima of this substrate in the lake, as e.g. found in the epilimnion in April 2015 (Fig. 1). The Put uptake rate at the highest

offered concentration (100 nM) was approximately 2 times V_{max} and thus significantly deviated from the fitted hyperbolic curve (Fig. 3a). This discrepancy could be explained by the results of our microautoradiographic analysis: the filamentous cyanobacterium *P. rubescens* (6 μg Chl *a* L^{-1} at 5 m depth in March 2016) was found to readily incorporate radiolabeled Put at 100 nM but not at 10 nM (Figs. 7g, h).

The uptake of polyamines by bacteria is mainly mediated via a putrescine-specific transport system and a second one that is preferential for spermidine (Tabor and Tabor 1985; Mou et al. 2010). Besides external sources, bacteria can also synthesize Put (and in turn also Spd) from arginine, ornithine or methionine (Tabor and Tabor 1984; 1985). Put uptake in *E. coli* was significantly inhibited upon addition of other polyamines and amino acids (such as ornithine), albeit at μM levels only (Tabor and Tabor 1966). Our competition assay with natural plankton assemblage illustrates that the addition of Spd entirely suppressed heterotrophic Put consumption, whereas the presence of both Put precursor amino acids (ornithine and arginine) did not affect its uptake, as compared to the control amended with Put only (Fig. 5). This confirms the presence of taxa harboring the spermidine-preferential uptake system in the plankton of Lake Zurich, which corresponds with findings from marine metatranscriptomes (Mou et al. 2011). Genes for the two major transport proteins were found in many phyla such as for example Proteobacteria, Cyanobacteria or Actinobacteria (Mou et al. 2010; Ghylin et al. 2014; Kurihara and Suzuki 2015). This suggests that numerous microorganisms harbor multiple parallel transport systems to regulate the uptake of different polyamines according to their actual availability, as reflected by our kinetic measurements (Fig. 4). Our data also document that heterotrophs did not select against putrescine in the presence of free amino acids suggesting a stable preference for polyamines. Moreover, a rapid decrease (50% over 5 h) in the Spd concentration during the competition assay implies

544 that the heterotrophic Spd uptake rate is comparable to that of Put. However, the negligible
545 Spd concentrations in Lake Zurich likely limit its importance to bacterioplankton consumers,
546 as previously reported for N-acetylglucosamine (Horňák and Pernthaler 2014).
547
548 *Identification of Put incorporating cells*
549 Despite measurable incorporation rates obtained with ^{14}C-Put (incubations I and II,
550 Table 2), no cells with visible Put assimilation could be detected by MAR (data not shown).
551 Thus, additional MAR analyses were performed using ^{3}H-Put, which yielded a specific MAR
552 signal clearly distinguishable from the negative controls. This discrepancy might be due to
553 the higher specific activity of the ^{3}H-labeled tracer (60 Ci mmol^{-1}) compared to the ^{14}C label
554 (110 mCi mmol^{-1}), likely resulting in a higher amount of silver grains in the near vicinity of
555 cells (Fig. 7).
556 Using MAR combined with CARD-FISH (Alonso and Pernthaler 2005) we provide
557 first direct evidence of Put assimilation at 10 nM concentration by different groups of
558 freshwater bacterioplankton (Figs. 6, 7). Moreover, the summed abundances of the individual
559 taxa of Put incorporating bacteria corresponded well to the fraction of all DAPI-stained
560 bacteria with positive MAR signals (11 %), indicating that we successfully identified the
561 large majority of Put assimilating planktonic bacteria. The highest fractions (20 – 30 %) of
562 Put incorporating cells were affiliated with the acI lineage of Actinobacteria and with
563 Betaproteobacteria, notably the R-BT lineage of the genus *Limnohabitans* (Fig. 6b). In
564 comparison, only 4 – 7 % of bacteria affiliated with the recently described LimA cluster of
565 the genus *Limnohabitans* (Shabarova et al. 2017) incorporated Put. The bacterioplankton
566 assemblage of Lake Zurich during the growing season is numerically dominated by
567 Actinobacteria and Betaproteobacteria (Salcher et al. 2008, 2013; Eckert et al. 2012), which

568 further emphasizes the quantitative importance of these groups as Put consumers. Our results
569 confirm the consumption of Put by members of the acI lineage of Actinobacteria, as
570 hypothesized from the reconstruction of the respective metabolic pathway in single-cell
571 amplified genomes (Ghylin et al. 2014). Genome sequences of *Limnohabitans planktonicus*
572 (Kasalický et al. 2010) and other *Limnohabitans* isolates (Zeng et al., 2012) also indicate the
573 presence of polyamine transporters. In contrast, no such uptake mechanism was found in
574 members of the *Polynucleobacter*-C cluster (Hahn et al. 2009, 2016) which agrees with our
575 MAR analyses. This points at differences in substrate preferences between these sympatric
576 betaproteobacterial lineages, as has been shown before for other labile DOC compounds
577 (Salcher et al. 2013). Other epilimnetic populations with fractions of active cells above the
578 community average (11%) were affiliated with Cyclobacteriaceae and Alphaproteobacteria
579 (Fig. 6b). However, the common freshwater alphaproteobacterial LD12 lineage (Salcher et al.
580 2011) did not show positive MAR signals, which may reflect their suggested oligotrophic
581 lifestyle. Therefore, lower Put concentrations (e.g. 1 nM) or longer incubation times should
582 be tested to confirm the MAR results of our study.

583 The planktonic diatom *Asterionella sp*. and the cyanobacterium *P. rubescens*
584 incorporated Put at 10 and 100 nM concentrations, respectively (Fig. 7e, h). This agrees with
585 previous reports on the uptake of diverse monomers by *P. rubescens* (e.g.: Zotina et al. 2003)
586 and diatoms (Tuchman et al. 2006), by which these primarily phototrophic organisms may
587 satisfy significant fractions of their nitrogen and carbon demands. In *Asterionella* sp., the
588 number of silver grains, which is roughly proportional to the amount of assimilated Put
589 (Horňák et al., 2012), visibly increased at 100 nM (Fig. 7f) suggesting a concentration-
590 dependent Put incorporation. It remains to be investigated whether diatoms can also
591 assimilate Put at the low ambient concentrations (<2 nM) that are more frequently

592 encountered in Lake Zurich. Finally, several bacterial taxa in the hypolimnion showed a
593 comparable potential for Put assimilation (Fig. 6), even though the in situ concentrations of
594 this substrate were much lower than in the epilimnion (Fig 1). As in the case of Spd
595 incorporation this again demonstrates a "preparadness" of bacterioplankton populations to
596 utilize a substrate despite its apparent rarity.

597

598 **References**

599 Alonso, C., and J. Pernthaler. 2005. Incorporation of glucose under anoxic conditions by
600 bacterioplankton from coastal North Sea surface waters. Appl. Environ. Microbiol. **71**:
601 1709–1716. doi:10.1128/aem.71.4.1709-1716.2005
602 Amann, R., F.-O. Glöckner, and A. Neef. 1997. Modern methods in subsurface microbiology:
603 in situ identification of microorganisms with nucleic acid probes. FEMS Microbiol. Rev.
604 **20**: 191–200. doi:10.1111/j.1574-6976.1997.tb00308.x
605 Badini, L., R. Pistocchi, and N. Bagni. 1994. Polyamine transport in the seaweed *Ulva rigida*
606 (Chlorophyta). J. Phycol. **30**: 599–605. doi:10.1111/j.0022-3646.1994.00599.x
607 Bertilsson, S., A. Eiler, A. Nordqvist, and N. O. G. Jørgensen. 2007. Links between bacterial
608 production, amino-acid utilization and community composition in productive lakes.
609 ISME J. **1**: 532–544. doi:10.1038/ismej.2007.64
610 Beutler, M., K. H. Wiltshire, B. Meyer, C. Moldaenke, C. Luring, M. Meyerhofer, U. P.
611 Hansen, and H. Dau. 2002. A fluorometric method for the differentiation of algal
612 populations in vivo and in situ. Photosynth. Res. **72**: 39–53.
613 doi:10.1023/a:1016026607048
614 Bossard, P., S. Gammeter, C. Lehmann, F. Schanz, R. Bachofen, H. R. Burgi, D. Steiner, and
615 U. Zimmermann. 2001. Limnological description of the Lakes Zurich, Lucerne, and
616 Cadagno. Aquat. Sci. **63**: 225–249. doi:10.1007/PL00001353
617 Burnison, B. K., and R. Y. Morita. 1974. Heterotrophic potential for amino acid uptake in a
618 naturally eutrophic lake. Appl. Microbiol. **27**: 488–495.
619 Crawford, C. C., J. E. Hobbie, and K. L. Webb. 1974. The utilization of dissolved free amino
620 acids by estuarine microorganisms. Ecology **55**: 551–563. doi:10.2307/1935146
621 Daims, H., A. Bruhl, R. Amann, K. H. Schleifer, and M. Wagner. 1999. The domain-specific

probe EUB338 is insufficient for the detection of all bacteria: development and evaluation of a more comprehensive probe set. Syst. Appl. Microbiol. **22**: 434–444. doi:10.1016/S0723-2020(99)80053-8

Eckert, E. M., M. M. Salcher, T. Posch, B. Eugster, and J. Pernthaler. 2012. Rapid successions affect microbial N-acetyl-glucosamine uptake patterns during a lacustrine spring phytoplankton bloom. Environ. Microbiol. **14**: 794–806. doi:10.1111/j.1462-2920.2011.02639.x

Feuillade, M., J. Feuillade, and V. Fiala. 1990. The effect of light on the release of organic compounds by the cyanobacterium *Oscillatoria rubescens*. Aquat. Sci. **52**: 345–359. doi:10.1007/BF00879762

Gao, S., S. Bhoopathy, Z.-P. Zhang, D. S. Wright, R. Jenkins, and H. T. Karnes. 2006. Evaluation of volatile ion-pair reagents for the liquid chromatography–mass spectrometry analysis of polar compounds and its application to the determination of methadone in human plasma. J. Pharm. Biomed. Anal. **40**: 679–688. doi:http://dx.doi.org/10.1016/j.jpba.2005.05.022

Garneau, M.-È., T. Posch, and J. Pernthaler. 2015. Seasonal patterns of microcystin-producing and non-producing *Planktothrix rubescens* genotypes in a deep pre-alpine lake. Harmful Algae **50**: 21–31. doi:10.1016/j.hal.2015.10.001

Ghylin, T. W., S. L. Garcia, F. Moya, and others. 2014. Comparative single-cell genomics reveals potential ecological niches for the freshwater acI Actinobacteria lineage. ISME J. **8**: 2503–2516. doi:10.1038/ismej.2014.135

Gosetti, F., E. Mazzucco, V. Gianotti, S. Polati, and M. C. Gennaro. 2007. High performance liquid chromatography/tandem mass spectrometry determination of biogenic amines in typical Piedmont cheeses. J. Chromatogr. A **1149**: 151–157. doi:http://dx.doi.org/10.1016/j.chroma.2007.02.097

Gosetti, F., E. Mazzucco, M. C. Gennaro, and E. Marengo. 2013. Simultaneous determination of sixteen underivatized biogenic amines in human urine by HPLC-MS/MS. Anal. Bioanal. Chem. **405**: 907–916. doi:10.1007/s00216-012-6269-z

Grossart, H., and M. Simon. 1998. Bacterial colonization and microbial decomposition of limnetic organic aggregates (lake snow). Aquat. Microb. Ecol. **15**: 127–140. doi:10.3354/ame015127

Hahn, M. W., E. Lang, U. Brandt, Q. L. Wu, and T. Scheuerl. 2009. Emended description of the genus *Polynucleobacter* and the species *P. necessarius* and proposal of two subspecies, *P. necessarius* subspecies *necessarius* subsp. nov. and *P. necessarius* subspecies *asymbioticus* subsp. nov. Int. J. Syst. Evol. Microbiol. **59**: 2002–2009. doi: 10.1099/ijs.0.005801-0

Hahn, M. W., J. Jezberová, U. Koll, T. Saueressig-Beck, and J. Schmidt. 2016. Complete ecological isolation and cryptic diversity in *Polynucleobacter* bacteria not resolved by 16S rRNA gene sequences. ISME J. **10**: 1642–1655. doi:10.1038/ismej.2015.237

Häkkinen, M. R., T. A. Keinänen, J. Vepsäläinen, A. R. Khomutov, L. Alhonen, J. Jänne, and S. Auriola. 2007. Analysis of underivatized polyamines by reversed phase liquid chromatography with electrospray tandem mass spectrometry. J. Pharm. Biomed. Anal. **45**: 625–634. doi:10.1016/j.jpba.2007.09.001

Häkkinen, M. R., A. Roine, S. Auriola, and others. 2013. Analysis of free, mono- and diacetylated polyamines from human urine by LC-MS/MS. J. Chromatogr. B-Analytical Technol. Biomed. Life Sci. **941**: 81–89. doi:10.1016/j.jchromb.2013.10.009

Hamana, K., and S. Matsuzaki. 1982. Widespread occurrence of norspermidine and norspermine in eukaryotic algae. J. Biochem. **91**: 1321–1328.

Hamana, K., and S. Matsuzaki. 1992. Polyamines as a chemotaxonomic marker in bacterial systematics. Crit. Rev. Microbiol. **18**: 261–283. doi:10.3109/10408419209113518

Höfle, M. G. 1984. Degradation of putrescine and cadaverine in seawater cultures by marine bacteria. Appl. Environ. Microbiol. **47**: 843–849.

Horňák, K., M. Zeder, J.F. Blom, T. Posch, and J. Pernthaler. 2012. Suboptimal light conditions negatively affect the heterotrophy of *Planktothrix rubescens* but are beneficial for accompanying *Limnohabitans* spp. Environ. Microbiol. **14**: 765–778. doi:10.1111/j.1462-2920.2011.02635.x

Horňák, K., and J. Pernthaler. 2014. A novel ion-exclusion chromatography-mass spectrometry method to measure concentrations and cycling rates of carbohydrates and amino sugars in freshwaters. J. Chromatogr. A **1365**: 115–123. doi:10.1016/j.chroma.2014.09.007

Horňák, K., H. Schmidheiny, and J. Pernthaler. 2016. High-throughput determination of dissolved free amino acids in unconcentrated freshwater by ion-pairing liquid

chromatography and mass spectrometry. J. Chromatogr. A **1440**: 85–93. doi:10.1016/j.chroma.2016.02.045

Igarashi, K., and K. Kashiwagi. 1999. Polyamine transport in bacteria and yeast. Biochem. J. **344**: 633–642. doi:10.1042/0264-6021:3440633

Igarashi, K., and K. Kashiwagi. 2000. Polyamines: Mysterious modulators of cellular functions. Biochem. Biophys. Res. Commun. **271**: 559–564. doi:10.1006/bbrc.2000.2601

Jantaro, S., P. Maenpaa, P. Mulo, and A. Incharoensakdi. 2003. Content and biosynthesis of polyamines in salt and osmotically stressed cells of *Synechocystis sp.* PCC 6803. FEMS Microbiol. Lett. **228**: 129–135. doi:10.1016/S0378-1097(03)00747-X

Johnson, K. A., and R. S. Goody. 2011. The original Michaelis constant: Translation of the 1913 Michaelis–Menten paper. Biochemistry **50**: 8264–8269. doi:10.1021/bi201284u

Jørgensen, N. O. G., M. Sondergaard, H. J. Hansen, S. Bosselmann, and B. Riemann 1983. Diel variation in concentration, assimilation and respiration of dissolved free amino acids in relation to primary and secondary production in two eutrophic lakes. Hydrobiologia **107**: 107–122. doi:10.1007/BF00017426

Jørgensen, N. O. G. 1992. Incorporation of [3H] leucine and [3H] valine into protein of freshwater bacteria: field applications. Appl. Environ. Microbiol. **58**: 3647–3653.

Kasalický, V., J. Jezbera, K. Šimek, and M. W. Hahn. 2010. *Limnohabitans planktonicus* sp. nov. and *Limnohabitans parvus* sp. nov., planktonic betaproteobacteria isolated from a freshwater reservoir, and emended description of the genus *Limnohabitans*. Int. J. Syst. Evol. Microbiol. **60**: 2710-2714. doi: 10.1099/ijs.0.018952-0

Kirchman, D. 2001. Measuring bacterial biomass production and growth rates from leucine incorporation in natural aquatic environments. Methods Microbiol. **30**: 227–237. doi:10.1016/s0580-9517(01)30047-8

Kuhlmann, F. E., A. Apffel, S. M. Fischer, G. Goldberg, and P. C. Goodley. 1995. Signal enhancement for gradient reverse-phase high-performance liquid chromatography electrospray ionization mass spectrometry analysis with trifluoroacetic and other strong acid modifiers by postcolumn addition of propionic acid and isopropanol. J. Am. Soc. Mass Spectrom. **6**: 1221–1225. doi:10.1016/1044-0305(95)00571-4

Kurihara, S.; Suzuki, H. 2015. Recent advances in bacterial polyamine transport systems, p.

171-178. In H. Kusano and T. Suzuki [eds.], Polyamines: a universal molecular nexus for growth, survival, and specialized metabolism. Springer.

Kusano, T., T. Berberich, C. Tateda, and Y. Takahashi. 2008. Polyamines: essential factors for growth and survival. Planta **228**: 367–381. doi:10.1007/s00425-008-0772-7

Lee, C., and N. O. G. Jørgensen. 1995. Seasonal cycling of putrescine and amino-acids in relation to biological production in a stratified coastal salt pond. Biogeochemistry **29**: 131–157.

Liu, Q., X. Lu, B. B. Tolar, X. Mou, and J. T. Hollibaugh. 2015. Concentrations, turnover rates and fluxes of polyamines in coastal waters of the South Atlantic Bight. Biogeochemistry **123**: 117–133.

Lu, X. X., L. Zou, C. Clevinger, Q. Liu, J. T. Hollibaugh, and X. Z. Mou. 2014. Temporal dynamics and depth variations of dissolved free amino acids and polyamines in coastal seawater determined by high-performance liquid chromatography. Mar. Chem. **163**: 36–44. doi:10.1016/j.marchem.2014.04.004

Lu, X., S. Sun, J. T. Hollibaugh, and X. Mou. 2015. Identification of polyamine-responsive bacterioplankton taxa in South Atlantic Bight. Environ. Microbiol. Rep. **7**: 831–838. doi:10.1111/1758-2229.12311

Manz, W., R. Amann, W. Ludwig, M. Wagner, and K.-H. Schleifer. 1992. Phylogenetic oligodeoxynucleotide probes for the major subclasses of Proteobacteria: problems and solutions. Syst. Appl. Microbiol. **15**: 593–600. doi:10.1016/S0723-2020(11)80121-9

Moran, M. A., R. Belas, M. A. Schell, and others. 2007. Ecological genomics of marine Roseobacters. Appl. Environ. Microbiol. **73**: 4559–4569. doi:10.1128/AEM.02580-06

Mou, X., S. Sun, P. Rayapati, and M. Moran. 2010. Genes for transport and metabolism of spermidine in *Ruegeria pomeroyi* DSS-3 and other marine bacteria. Aquat. Microb. Ecol. **58**: 311–321. doi:10.3354/ame01367

Mou, X. Z., M. Vila-Costa, S. L. Sun, W. D. Zhao, S. Sharma, and M. A. Moran. 2011. Metatranscriptomic signature of exogenous polyamine utilization by coastal bacterioplankton. Environ. Microbiol. Rep. **3**: 798–806. doi:10.1111/j.1758-2229.2011.00289.x

Nagata, T. 2000. Production mechanisms of dissolved organic matter, p. 121–152. In D. L. Kirchman [ed.], Microbial ecology of the ocean. Wiley-Liss.

746 Neuenschwander, S. M., M. M. Salcher, and J. Pernthaler. 2015. Fluorescence in situ
747 hybridization and sequential catalyzed reporter deposition (2C-FISH) for the flow
748 cytometric sorting of freshwater ultramicrobacteria. Front. Microbiol. **6**.
749 doi:24710.3389/fmicb.2015.00247
750 Nishibori, N. 2001. Detection of free polyamine in coastal seawater using ion exchange
751 chromatography. ICES J. Mar. Sci. **58**: 1201–1207. doi:10.1006/jmsc.2001.1115
752 Nishibori, N., Y. Matuyama, T. Uchida, T. Moriyama, Y. Ogita, M. Oda, and H. Hirota.
753 2003. Spatial and temporal variations in free polyamine distributions in Uranouchi Inlet,
754 Japan. Mar. Chem. **82**: 307–314. doi:10.1016/s0304-4203(03)00076-8
755 Nishibori, N., and T. Nishijima. 2004. Changes in polyamine levels during growth of a red-
756 tide causing phytoplankton *Chattonella antiqua* (*Raphidophyceae*). Eur. J. Phycol. **39**:
757 51–55. doi:10.1080/09670260310001636677
758 Nishibori, N., M. Niitsu, S. Fujihara, T. Sagara, S. Nishio, and I. Imai. 2009. Occurrence of
759 the polyamines caldopentamine and homocaldopentamine in axenic cultures of the red
760 tide flagellates *Chattonella antiqua* and *Heterosigma akashiwo* (*Raphidophyceae*).
761 FEMS Microbiol. Lett. **298**: 74–78. doi:10.1111/j.1574-6968.2009.01701.x
762 Pernthaler, J., E. Zollner, F. Warnecke, and K. Jürgens. 2004. Bloom of filamentous bacteria
763 in a mesotrophic lake: identity and potential controlling mechanism. Appl. Environ.
764 Microbiol. **70**: 6272–6281. doi:10.1128/AEM.70.10.6272-6281.2004
765 Posch, T., B. Eugster, F. Pomati, J. Pernthaler, G. Pitsch, and E. Eckert. 2015. Network of
766 interactions between ciliates and phytoplankton during spring. Front. Microbiol. **6**:
767 1289. doi: 10.3389/fmicb.2015.01289
768 Salcher, M. M., J. Pernthaler, M. Zeder, R. Psenner, and T. Posch. 2008. Spatio-temporal
769 niche separation of planktonic Betaproteobacteria in an oligo-mesotrophic lake. Environ.
770 Microbiol. **10**: 2074–2086. doi:10.1111/j.1462-2920.2008.01628.x
771 Salcher, M. M., J. Pernthaler, and T. Posch. 2011. Seasonal bloom dynamics and
772 ecophysiology of the freshwater sister clade of SAR11 bacteria “that rule the waves”
773 (LD12). ISME J. **5**: 1242–1252. doi:10.1038/ismej.2011.8
774 Salcher, M. M., T. Posch, and J. Pernthaler. 2013. In situ substrate preferences of abundant
775 bacterioplankton populations in a prealpine freshwater lake. ISME J. **7**: 896–907.
776 doi:10.1038/ismej.2012.162

Sekar, R., A. Pernthaler, J. Pernthaler, F. Warnecke, T. Posch, and R. Amann. 2003. An improved protocol for quantification of freshwater Actinobacteria by fluorescence in situ hybridization. Appl. Environ. Microbiol. **69**: 2928–2935. doi:10.1128/AEm.69.5.2928-2935.2003

Shabarova, T., V. Kasalický, K. Šimek, J. Nedoma, P. Znachor, T. Posch, J. Pernthaler, and M. M. Salcher. 2017. Distribution and ecological preferences of the freshwater lineage LimA (genus *Limnohabitans)* revealed by a new double hybridisation approach. Environ. Microbiol. doi:10.1111/1462-2920.13663

Šimek, K., J. Pernthaler, M. G. Weinbauer, K. Horňák, J. R. Dolan, J. Nedoma, M. Mašín, and R. Amann. 2001. Changes in bacterial community composition and dynamics and viral mortality rates associated with enhanced flagellate grazing in a mesoeutrophic reservoir. Appl. Environ. Microbiol. **67**: 2723–2733. doi:10.1128/AEM.67.6.2723-2733.2001

Simon, M., and M. M. Tilzer. 1987. Bacterial response to seasonal changes in primary production and phytopplankton biomass in Lake Constance. J. Plankt. Res. **9**: 535–552. doi:org/10.1093/plankt/9.3.535

Sirocchi, V., G. Caprioli, M. Ricciutelli, S. Vittori, and G. Sagratini. 2014. Simultaneous determination of ten underivatized biogenic amines in meat by liquid chromatography-tandem mass spectrometry (HPLC-MS/MS). J. Mass Spectrom. **49**: 819–825. doi:10.1002/jms.3418

Tabor, C. W., and H. Tabor. 1966. Transport systems for 1,4-diaminobutane, spermidine, and spermine in Escherichia coli. J. Biol. Chem. **241**: 3714–3723.

Tabor, C. W., and H. Tabor. 1984. Polyamines. Annu. Rev. Biochem. **53**: 749–790. doi:10.1146/annurev.bi.53.070184.003533

Tabor, C. W., and H. Tabor. 1985. Polyamines in Microorganisms. Microbiol. Rev. **49**: 81–99.

Tuchman, N. C., M. A. Schollett, S. T. Rier, and P. Geddes. 2006. Differential heterotrophic utilization of organic compounds by diatoms and bacteria under light and dark conditions. Hydrobiologia **561**: 167–177. doi:10.1007/s10750-005-1612-4

Warnecke, F., R. Sommaruga, R. Sekar, J. S. Hofer, and J. Pernthaler. 2005. Abundances, identity, and growth state of actinobacteria in mountain lakes of different UV

transparency. Appl. Environ. Microbiol. **71**: 5551–5559. doi:10.1128/AEM.71.9.5551-5559.2005

Weiss, M., and M. Simon. 1999. Consumption of labile dissolved organic matter by limnetic bacterioplankton: the relative significance of amino acids and carbohydrates. Aquat. Microb. Ecol. **17**: 1–12. doi:10.3354/ame017001

Yankova, Y., J. Villiger, J. Pernthaler, F. Schanz, and T. Posch. 2016. Prolongation, deepening and warming of the metalimnion change habitat conditions of the harmful filamentous cyanobacterium *Planktothrix rubescens* in a prealpine lake. Hydrobiologia **776**: 125–138. doi:10.1007/s10750-016-2745-3

Zeder, M., E. Kohler, and J. Pernthaler. 2010. Automated quality assessment of autonomously acquired microscopic images of fluorescently stained bacteria. Cytometry. A **77**: 76–85. doi:10.1002/cyto.a.20810

Zeng, Y., V. Kasalický, K. Šimek, and M. Koblížek. 2012. Genome sequences of two freshwater proteobacterial isolates, *Limnohabitans* species strains Rim28 and Rim47, indicate their capabilities as both photoautotrophs and ammonia oxidizers. J. Bacteriol. **194**: 6302–6303. doi: 10.1128/JB.01481-12

Zotina, T., O. Köster, and F. Jüttner. 2003. Photoheterotrophy and light-dependent uptake of organic and organic nitrogenous compounds by *Planktothrix rubescens* under low irradiance. Freshw. Biol. **48**: 1859–1872. doi:10.1046/j.1365-2427.2003.01134.x

Acknowledgements:

We thank E. Loher, D. Marty and T. Posch for their help with sampling, chlorophyll *a* measurements and flow cytometry. Two anonymous reviewers and R. Howarth are acknowledged for their valuable comments on the earlier version of the manuscript. The study was supported by the Swiss National Science Foundation under the project 31003A-163217.

834 **Figure Legends:**

835 **Fig. 1:** (a) Spatiotemporal distribution of total DFPA concentrations (nM) in Lake Zurich
836 from February to October 2015. (b) Concentrations of individual DFPA from one selected
837 sampling date in each season (indicated by vertical dashed lines) of 2015. Dap =
838 diaminopropane, Put = putrescine, Spd = spermidine, Spm = spermine, Nsd = norspermidine
839
840 **Fig. 2:** Concentrations of (a) *Planktothrix rubescens*, (b) diatoms (both as μg Chl *a* L^{-1}), and
841 (c) total bacterial abundances (10^6 cells mL^{-1}) in the upper 25 m of Lake Zurich from
842 February to October 2015. Data is scaled to the maximum of the corresponding parameter.
843
844 **Fig. 3:** Temporal changes in concentrations of natural (^{12}C-Put) and isotopically labeled
845 putrescine (^{13}C-Put) in selected incubation experiments (I, II, and V) conducted with
846 unfiltered epilimnetic samples (5 m) from Lake Zurich during September 2015 (a, b) and July
847 2016 (c). Controls (Ctrl) that were not amended with ^{13}C-Put show concentrations of natural
848 putrescine only. Values are means of triplicates. Error bars show standard deviations.
849
850 **Fig. 4:** (a) ^{13}C-putrescine uptake rate as a function of its concentration in unfiltered samples
851 taken from Lake Zurich on 18 March 2016. The hyperbolic curve following the Michaelis-
852 Menten kinetics is fitted to data obtained from a 2 h incubation period. V_{max} = maximum
853 uptake rate. K_m = half saturation constant. Values are means of triplicates. Error bars show
854 relative standard deviations. (b) The corresponding double reciprocal (Lineweaver-Burk)
855 plot.
856

Fig. 5: Time-course of ^{13}C-labeled putrescine (^{13}C-Put) concentrations in eplimnetic samples (5 m) collected on 18 March 2016. Samples were amended with ^{13}C-Put or with a mixture of ^{13}C-Put and either arginine (Arg), ornithine (Orn), and spermidine (Spd). Arg, Orn, and Spd were added at 100 nM each. Values are means of triplicates. Error bars show standard deviations.

Fig. 6: (a) Relative abundances (as % of DAPI-stained cells) and (b) fractions of cells with visible putrescine incorporation (as % of hybridized cells) affiliated with Betaproteobacteria (BET), the R-BT lineage of the genus *Limnohabitans* (RBT); the LimA lineage of the genus *Limnohabitans* (LimA), the acI lineage of Actinobacteria (acI), Alphaproteobacteria (ALF), and Cyclobacteriaceae (Cyc). Values are means of triplicates. Error bars show standard deviations. A horizontal dashed line indicates the average Put incorporation (as % of DAPI-stained cells).

Fig. 7: Micrographs of cells assayed by MAR-FISH. Red colour indicates hybridized bacterial cells (a-d) or chlorophyll *a* autofluorescence (e-h) and blue colour DAPI-stained cells. Active putrescine incorporation is indicated by dark silver grains in near vicinity of cells. (a) acI lineage of Actinobacteria; (b) Betaproteobacteria, (c) Alphaproteobacteria; (d) Cyclobacteriaceae, (e) diatom *Asterionella sp.* incubated with 10 and (f) 100 nM ^{3}H-putrescine, (g) cyanobacterium *Planktothrix rubescens* incubated with 10 and (h) 100 nM ^{3}H-putrescine. All bacteria were incubated with 10 nM ^{3}H-putrescine. Scale bars show 5 µm (a-d) and 50 µm (e-h), respectively. Images were adjusted for brightness, contrast and colour saturation.

880 **Tables:**

881 **Table 1:** Overview of experimental incubations with stable isotope- and radiolabeled
882 putrescine performed with samples from Lake Zurich during 2015-2016. Samples were taken
883 from the depths of 5 and 120 m and incubated in triplicates for 2-5 h in the dark as unfiltered
884 (raw) or after filtration (<0.8 μm). Samples were amended with 10 nM of either ^{13}C- or
885 ^{14}C/^{3}H-labeled putrescine. Additional samples spiked with variable concentrations of ^{13}C- (1-
886 100 nM) or ^{3}H-labeled putrescine (10, 100 nM) were incubated on 18 March 2016. Cells with
887 visible putrescine incorporation were detected by microautoradiography (MAR) or by
888 microautoradiography combined with CARD-FISH (MAR-FISH). MAR preparations were
889 exposed for 1.5-2.5 days in the dark. *samples were incubated with putrescine (10 nM) or
890 with a mixture of putrescine (10 nM) and either ornithine, arginine, and spermidine (100 nM
891 each), nd – not determined

Table 1:

Incubation / Experiment	Date	Depth (m)	Sample	^{13}C -labeled putrescine			^{14}C/^{3}H-labeled putrescine		
				Volume (mL)	Concentration (nM)	Period (h)	Concentration (nM)	Detection	Exposure (d)
I / Uptake	24 Sept. 2015	5	raw	1000	10	0-5	10	^{14}C-MAR	1.5
II / Uptake	30 Sept. 2015	5	raw	1000	10	0-5	10	^{14}C-MAR	1.5
III / Kinetics	18 March 2016	5	raw	100	10* 1, 2, 5, 10, 20, 50, 100	0-4 0-2	10, 100	^{3}H-MAR-FISH	1.5
IV / MAR-FISH	27 April 2016	5, 120	raw	1000	10	0-4	10	^{3}H-MAR-FISH	2.5
V / Uptake	6 July 2016	5	raw <0.8 μm	250	10	0-4	10	nd	nd

892 **Table 2:** Putrescine in situ concentrations, uptake and incorporation rates, fractions of
893 incorporated putrescine and turnover times at the initial phase (0-2 h) of incubation
894 experiments. Note that putrescine incorporation rates were measured using ^{14}C- and ^{3}H-
895 labeled tracer in uptake experiments I-II and III-IV, respectively. *incorporation rates
896 measured with ^{3}H-tracer; nd – not determined.

Incubation/ Experiment	Date	Concentration (nM)	Uptake rate (nM h^{-1})	Incorporation rate (pM h^{-1})	Incorporated fraction (%)	Turnover time (h)
I / Uptake	24 Sept. 2015	2.2	5.0	901.6	18	2.4
II / Uptake	30 Sept. 2015	2.8	4.4	825.7	19	2.9
III / Kinetics	18 March 2016	2	3.7	22*	nd	3.2
IV / MAR-FISH	27 April 2016	1.7 (5 m)	3.2	15.5*	nd	3.7
		0.5 (120 m)	3.4	4.2*	nd	3
V / Uptake	6 July 2016	12 (raw)	5.0	36.7*	nd	4.4
		2.9 (<0.8 μm)	3.3	34.2*	nd	3.9

Figures:

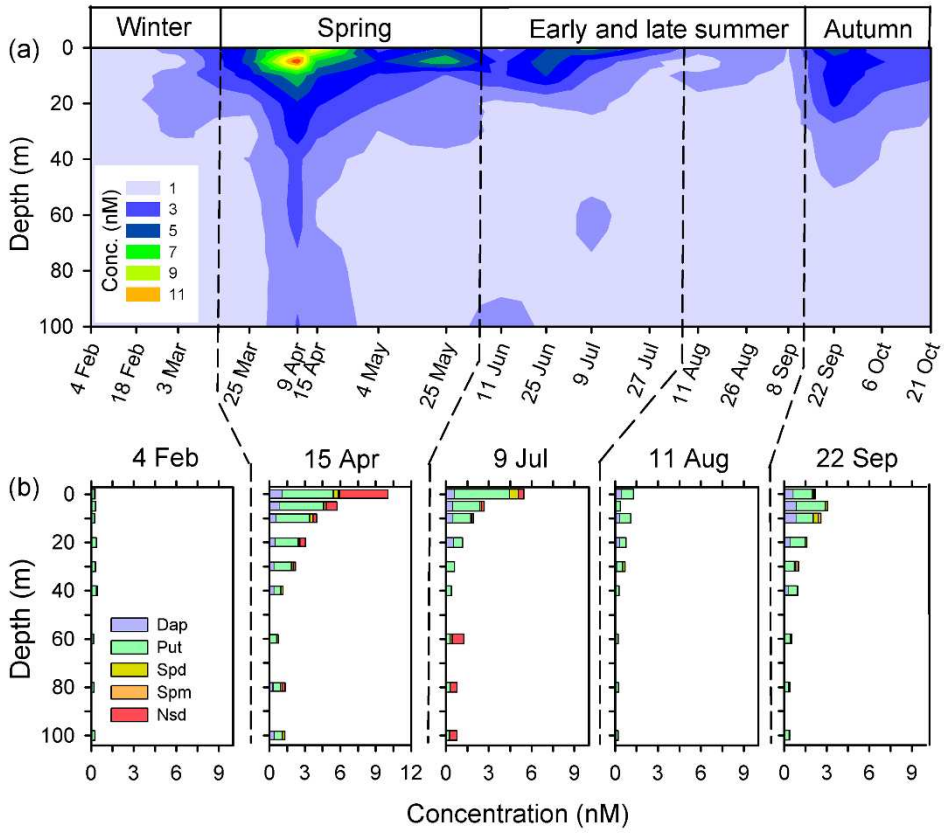

Fig. 1

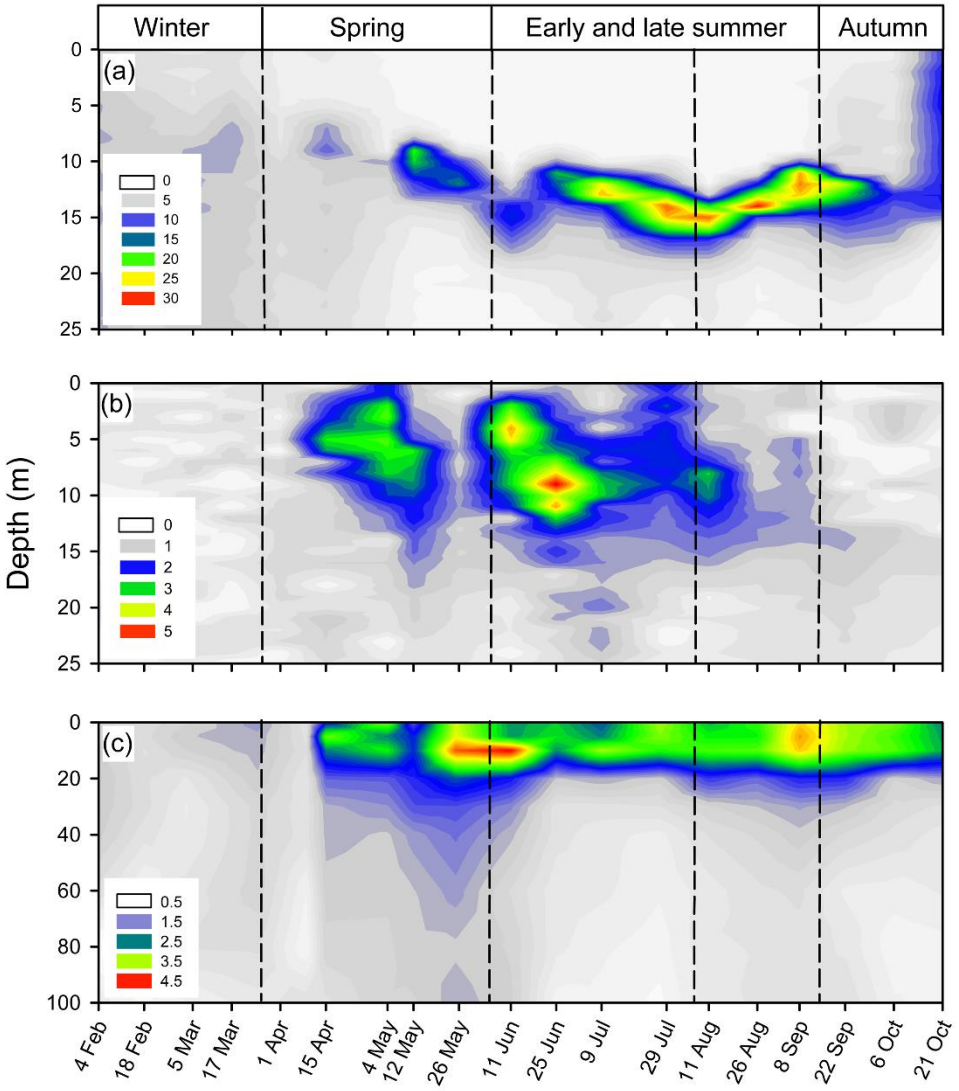
Winter
Spring
Early and late summer
Autumn
(a)
0
5
10
15
20
25
30
(b)
0
1
2
3
4
5
(c)
0.5
1.5
2.5
3.5
4.5
Depth (m)
0
5
10
15
20
25
0
20
40
60
80
100
4 Feb
18 Feb
5 Mar
17 Mar
1 Apr
15 Apr
4 May
12 May
26 May
11 Jun
25 Jun
9 Jul
29 Jul
11 Aug
26 Aug
8 Sep
22 Sep
6 Oct
21 Oct

Fig. 2

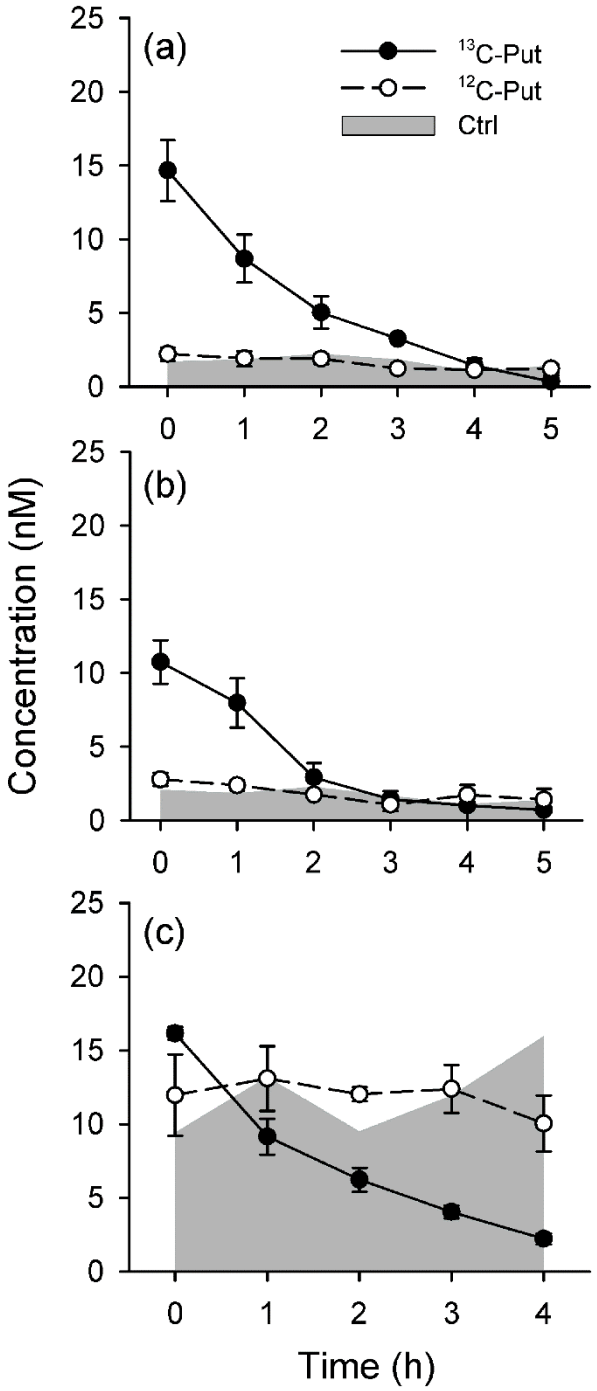
(a)
(b)
(c)
^{13}C-Put
^{12}C-Put
Ctrl
Concentration (nM)
Time (h)
0
5
10
15
20
25
0
1
2
3
4
5

Fig. 3

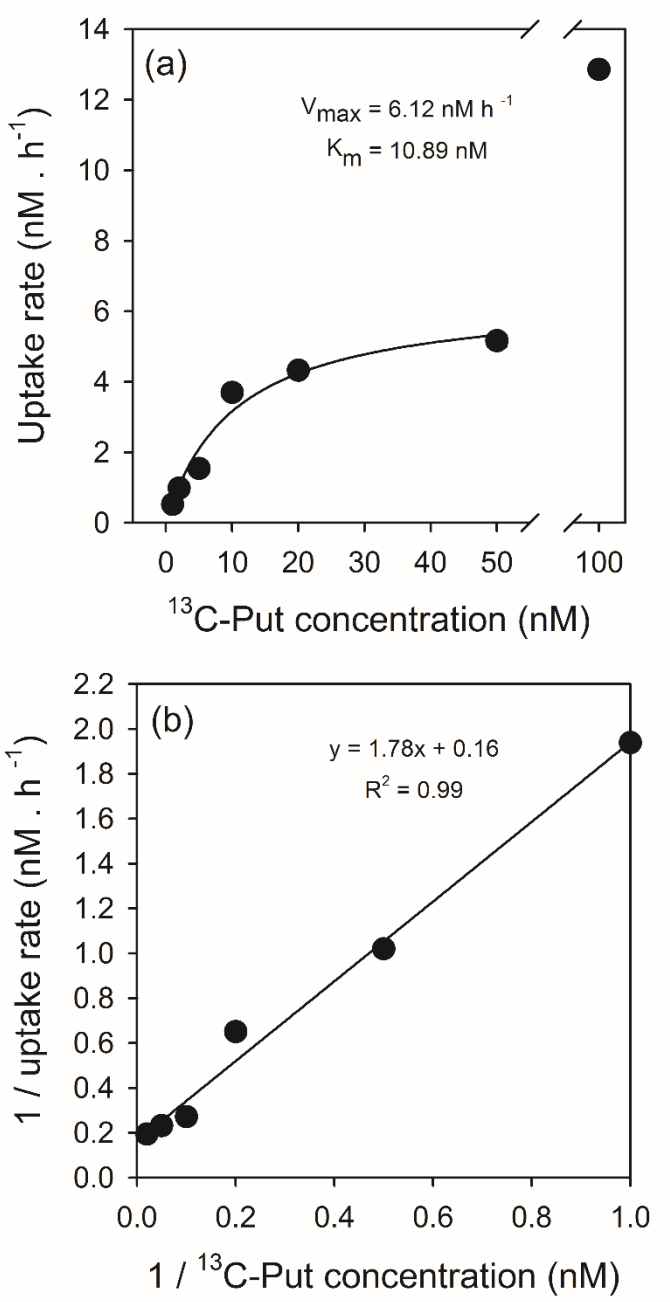
(a)
V_{max} = 6.12 nM h^{-1}
K_m = 10.89 nM
Uptake rate (nM . h^{-1})
^{13}C-Put concentration (nM)
(b)
y = 1.78x + 0.16
R^2 = 0.99
1 / uptake rate (nM . h^{-1})
1 / ^{13}C-Put concentration (nM)

Fig. 4

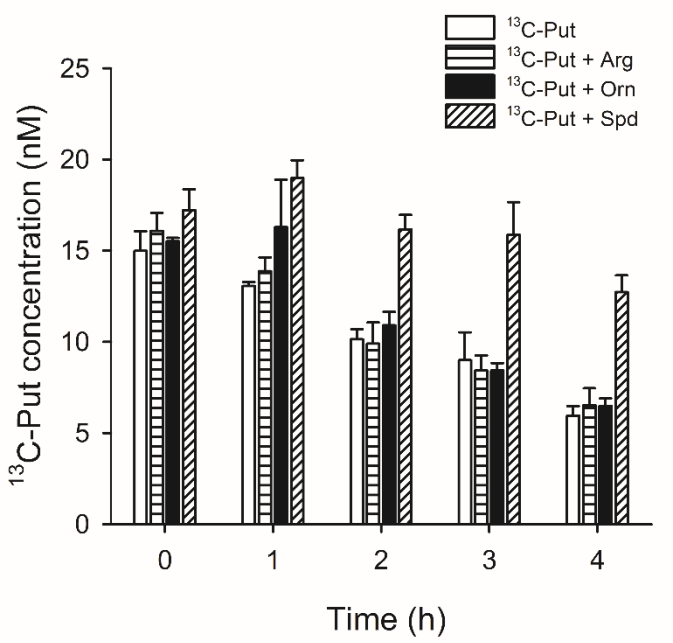
^{13}C-Put
^{13}C-Put + Arg
^{13}C-Put + Orn
^{13}C-Put + Spd
^{13}C-Put concentration (nM)
25
20
15
10
5
0
0
1
2
3
4
Time (h)

Fig. 5

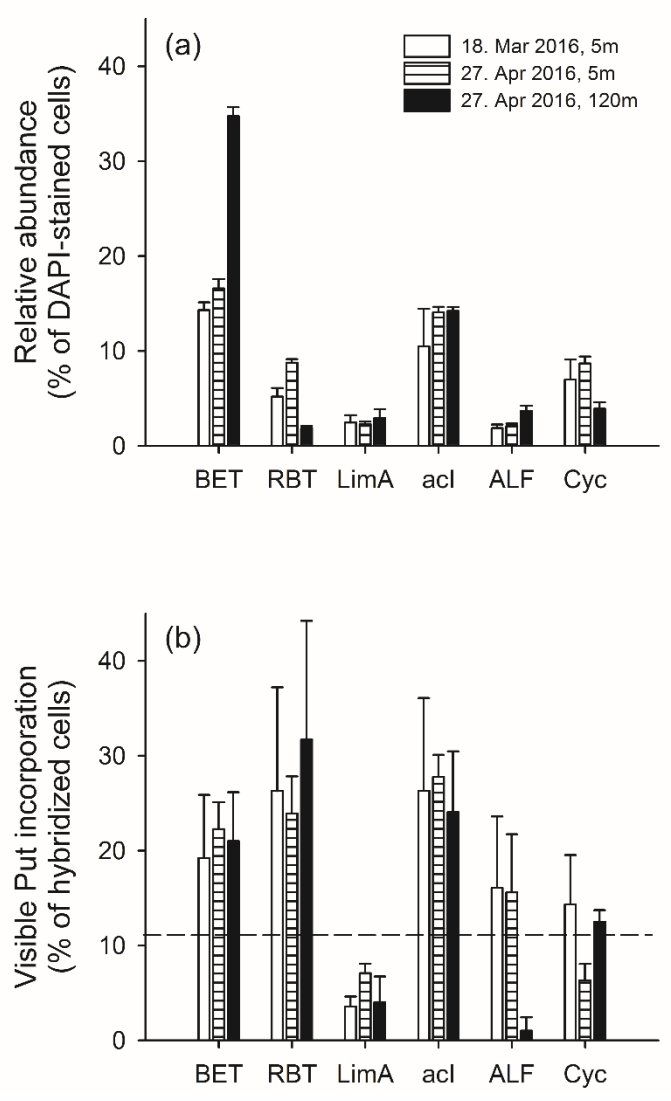
(a)
18. Mar 2016, 5m
27. Apr 2016, 5m
27. Apr 2016, 120m
Relative abundance
(% of DAPI-stained cells)
0
10
20
30
40
BET
RBT
LimA
acI
ALF
Cyc
(b)
Visible Put incorporation
(% of hybridized cells)
0
10
20
30
40
BET
RBT
LimA
acI
ALF
Cyc

Fig. 6

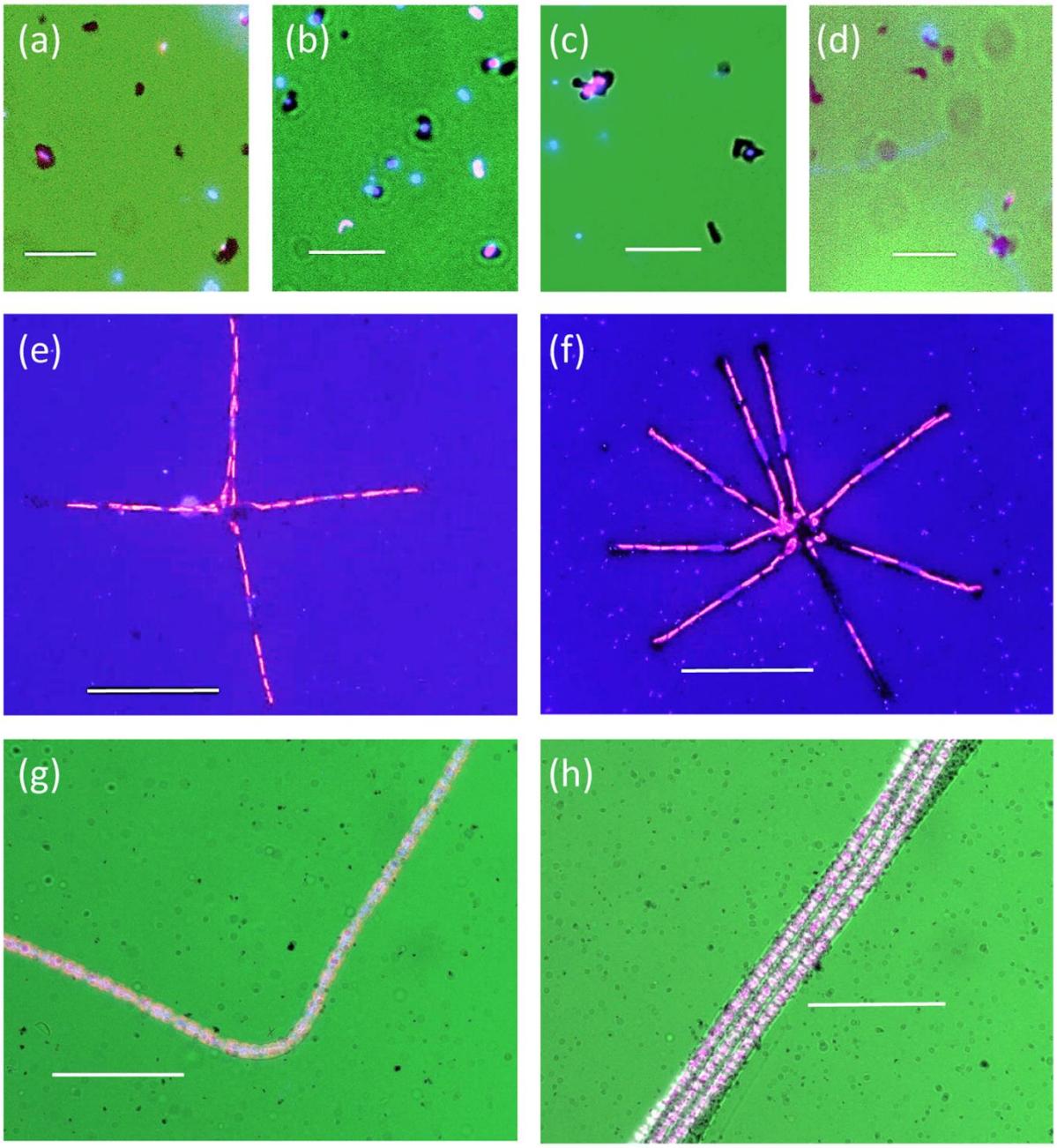

Fig. 7

Supplemental Information

Suppl. Table 1: Structures, formulas and molar masses of polyamines used in this study.

Polyamine	Structure	Formula	Molar mass (g mol^{-1})
diaminopropane	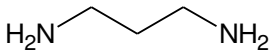	$C_3H_{10}N_2$	74.13
putrescine	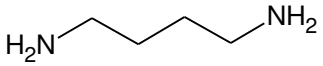	$C_4H_{12}N_2$	88.15
cadaverine	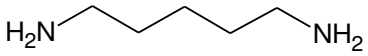	$C_5H_{14}N_2$	102.18
diaminoheptane	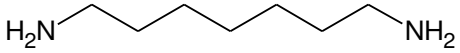	$C_7H_{18}N_2$	130.23
norspermidine	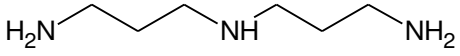	$C_6H_{17}N_3$	131.22
spermidine	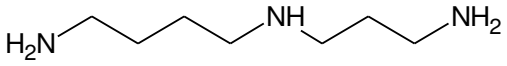	$C_7H_{19}N_3$	145.25
spermine	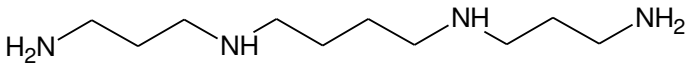	$C_{10}H_{26}N_4$	202.35

Suppl. Table 2: Mass spectrometry parameters for detection of polyamines. Transitions (pairs of precursor and product ions) and the corresponding declustering potential (DP), collision energy (CE), cell exit potential (CXP) parameters, limits of detection (LOD) and quantification (LOQ). Dap = diaminopentane, Put = putrescine, Cad = cadaverine, Dah = diaminoheptane, Nsd = norspermidine, Spd = spermidine, Spm = spermine, IS = internal standard. Transitions used for quantification are highlighted in bold. nd = not determined

Compound	DP (V)	Transitions (m/z)	CE (V)	CXP (V)	LOD (nM)	LOQ (nM)
Dap	60	**75/58**	15	15	0.2	1.0
Put	20	**89/72**	15	15	0.2	0.5
		89/31	35	14	nd	nd
^{13}C-Put	20	**93/76**	15	15	0.5	1.0
		93/32	35	14	nd	nd
Cad	20	**103/86**	15	18	0.2	0.5
		103/69	25	18	nd	nd
Dah (IS)	90	**131/114**	16	15	nd	nd
Nsd	50	**132/115**	17	15	0.1	1.0
		132/98	22	20	nd	nd
Spd	70	**146/112**	20	20	0.05	0.5
		146/129	15	28	nd	nd
Spm	70	**203/129**	17	18	0.1	1.0
		203/112	28	20	nd	nd

Suppl. Table 3: DFPA concentrations in surface samples from different habitats on 18 February 2016 and the corresponding recovery (means of duplicates ± range) measured with ^{13}C-labeled putrescine added to samples at 1 and 10 nM levels. Dap = diaminopropane, Put = putrescine, Nsd = norspermidine, Spd = spermidine, Spm = spermine, nd = not determined

Habitat	Dap (nM)	Put (nM)	Nsd (nM)	Spd (nM)	Spm (nM)	Recovery (%) 1 nM / 10 nM
Lake Zurich	2.5	18.8	0.3	1.3	0.3	101 ± 4 / 97 ± 3
Türlersee	2.3	9.5	0.1	0.5	0.2	90 ± 12 / 98 ± 1
Hüttnersee	1.5	10.4	0.2	0.7	0.1	124 ± 5 / 123 ± 3
Thalwiler Waldweiher	1.7	10.6	0.1	0.6	0.1	108 ± 4 / 101 ± 9
Seleger Moor	0.2	0.5	nd	1.4	0.1	121 ± 20 / 109 ± 5

Suppl. Fig. 1: Ion chromatograms of (a) a mixture of 7 polyamines (20 nM each) in Milli-Q water, and (b) a biomass extract from the planktonic diatom *Fragilaria sp.* isolated from Lake Zurich. Dap: diaminopropane, Put: putrescine, ^{13}C-Put: ^{13}C-putrescine, Cad: cadaverine, Nsd: norspermidine, Spd: spermidine, Spm: spermine, Dah: diaminoheptane (internal standard).

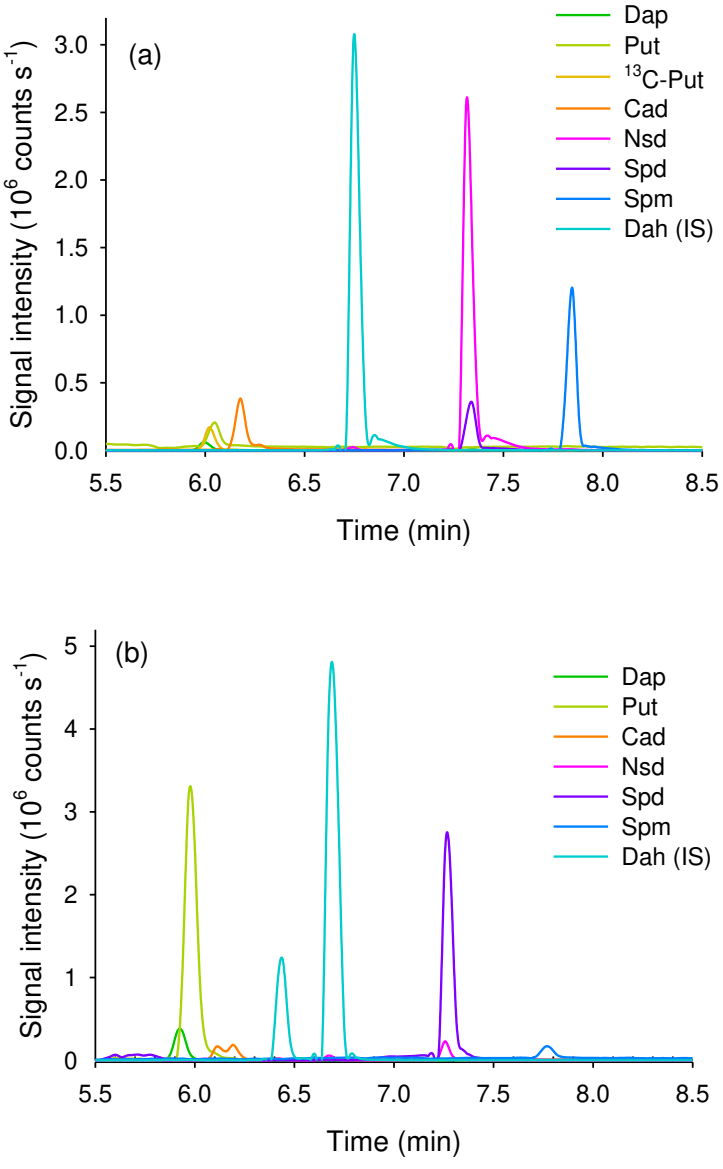

Suppl. Fig. 2: Signal intensities of selected pairs of precursor and product ions (transitions) specific to norspermidine (Nsd), spermidine (Spd) and putrescine (Put) as a function of their concentration (0.2 – 100 nM, note a logarithmic scale of the x-axis). Signal intensity of Nsd and Spd did not increase at concentrations >50 nM due to detector saturation indicated by a horizontal dashed line, whereas a continuous increase in signal intensity was observed for Put. Values are means of 3 replicates. Error bars show standard deviation.

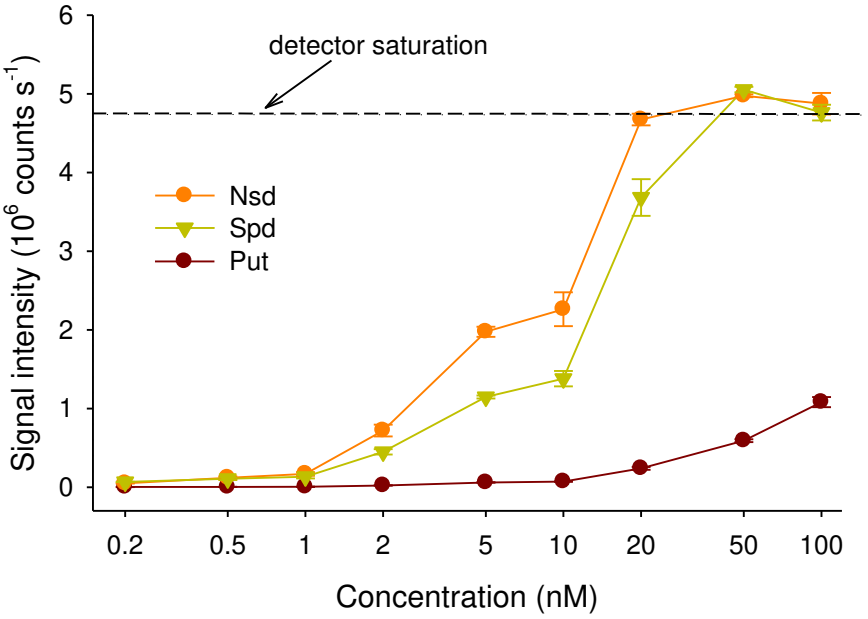

Suppl. Fig. 3: Temporal changes in the concentrations of natural (^{12}C-Put) and isotopically labeled putrescine (^{13}C-Put) in incubation experiment V conducted with filtered (0.8 μm membrane) epilimnetic samples (5 m) from Lake Zurich in July 2016. ^{13}C-Put was amended at a concentration of 10 nM. Controls that were not amended with ^{13}C-Put show concentrations of natural putrescine only. Values are means of 3 replicates. Error bars show standard deviation (range is shown for controls).